MICROCOPY RESOLUTION TEST CHART
NATIONAL BUREAU OF STANDARDS – 1963

DTIC FILE COPY

AD-A187 779

# NAVAL POSTGRADUATE SCHOOL
## Monterey, California

DTIC
ELECTE
JAN 0 7 1988
S    D

---

NORTHERN WINTER CIRCULATIONS FOR THE PERIOD
1974-1983

James S. Boyle
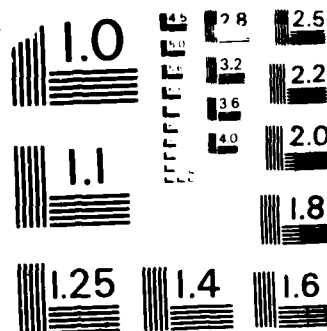
C.-P. Chang

Technical Report Period: Aug 1986-Aug 1987

---

87  12  14  115
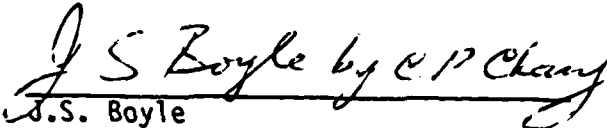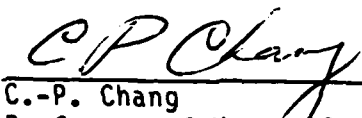
NAVAL POSTGRADUATE SCHOOL
Monterey, California

Rear Admiral R. Austin                          K. Marshall
Superintendent                                  Provost (Acting)

This report was prepared by:


_J.S. Boyle by C P Chang_  _C P Chang_
J.S. Boyle                                      C.-P. Chang
Adjunct Professor of Meteorology                Professor of Meteorology
Department of Meteorology                       Department of Meteorology
                                                (408) 646-2840


Publication of the report does not constitute approval of the sponsor for the findings or conclusions. It is published for information and for the exchange and stimulation of ideas.


Reviewed by:                                    Released by:


Robert J. Renard                                Gordon E. Schacher
Chairman                                        Dean of Science and Engineering
Department of Meteorology

# REPORT DOCUMENTATION PAGE

ADA187779

| 1a REPORT SECURITY CLASSIFICATION | 1b RESTRICTIVE MARKINGS |
|---|---|
| Unclassified | None |

| 2a SECURITY CLASSIFICATION AUTHORITY | 3 DISTRIBUTION/AVAILABILITY OF REPORT |
|---|---|
| | Approved for public release; distribution is unlimited. |
| 2b DECLASSIFICATION/DOWNGRADING SCHEDULE | |

| 4 PERFORMING ORGANIZATION REPORT NUMBER(S) | 5 MONITORING ORGANIZATION REPORT NUMBER(S) |
|---|---|
| NPS-63-87-005 | |

| 6a NAME OF PERFORMING ORGANIZATION | 6b OFFICE SYMBOL (If applicable) | 7a NAME OF MONITORING ORGANIZATION |
|---|---|---|
| Dept. of Meteorology Naval Postgraduate Schl | 63 | |

| 6c ADDRESS (City, State, and ZIP Code) | 7b ADDRESS (City, State, and ZIP Code) |
|---|---|
| Dept. of Meteorology NPS, Code 63By Monterey, CA 93943 | |

| 8a NAME OF FUNDING/SPONSORING ORGANIZATION | 8b OFFICE SYMBOL (If applicable) | 9 PROCUREMENT INSTRUMENT IDENTIFICATION NUMBER |
|---|---|---|
| NOAA Climate Analysis Ctr | | 40AAW503656 |

| 8c ADDRESS (City, State, and ZIP Code) | 10 SOURCE OF FUNDING NUMBERS | | | |
|---|---|---|---|---|
| NOAA/CAC NMC Washington, DC 20233 | PROGRAM ELEMENT NO | PROJECT NO | TASK NO | WORK UNIT ACCESSION NO |
| | | | | |

11 TITLE (Include Security Classification)

Northern Winter Circulations for the Period 1974-1983

12 PERSONAL AUTHOR(S)
James S. Boyle and C.-P. Chang

| 13a TYPE OF REPORT | 13b TIME COVERED | 14 DATE OF REPORT (Year, Month, Day) | 15 PAGE COUNT |
|---|---|---|---|
| Technical | FROM 8/86 TO 8/87 | 30 November 1987 | 86 |

16 SUPPLEMENTARY NOTATION

| 17 COSATI CODES | | | 18 SUBJECT TERMS (Continue on reverse if necessary and identify by block number) |
|---|---|---|---|
| FIELD | GROUP | SUB-GROUP | |
| | | | atmospheric |
| | | | |

19 ABSTRACT (Continue on reverse if necessary and identify by block number)

This is the final report of the study on the winter circulation for the decade 1974-1983. The report consists of two parts:

Part I is an Observational study of the time mean flow and transients for the northern wintertime for the period 1974/5 to 1982/3. and

Part II is an Observational study of the divergent flow for the tropics and midlatitudes in the northern wintertime for the period 1974/5 to 1982/3. Keywords: Jet streams, Winter storms, Global geographical distributions, Synoptic meteorology, Transient Kinetic energy fields, Eddies (Fluid mechanics); Vortices; Northern hemisphere.

| 20 DISTRIBUTION/AVAILABILITY OF ABSTRACT | 21 ABSTRACT SECURITY CLASSIFICATION |
|---|---|
| ☒ UNCLASSIFIED/UNLIMITED ☐ SAME AS RPT ☐ DTIC USERS | Unclassified |

| 22a NAME OF RESPONSIBLE INDIVIDUAL | 22b TELEPHONE (Include Area Code) | 22c OFFICE SYMBOL |
|---|---|---|
| James S. Boyle | (408) 646-3275 | 63By |

DD FORM 1473, 84 MAR     83 APR edition may be used until exhausted     SECURITY CLASSIFICATION OF THIS PAGE
All other editions are obsolete

# Table of Contents

A-1

i

# LIST OF FIGURES

ii

# ABSTRACT

This report consists of two parts: Part 1, Observational study of the time mean flow on transients for the northern wintertime for the period 1975/6 to 1982/3, and Part 2, Observational study of the divergent flow for the tropics and midlatitudes in the northern wintertime for the period 1974/5 to 1982/3. The research uses data from the tropical global band analysis produced by the Fleet Numerical Oceanography Center.

# Part 1

## Observational study of the time mean·flow

## and transients

## for the northern wintertime

### for the period 1974/75 to 1982/83

## ABSTRACT

A nine year data set of U. S. Navy operational, twice-daily wind analyses at 200 mb, 700 mb and the surface from $60°N$ to $40°S$ is used to compute statistics on the time mean fields and transient activity during the northern winter(December, January, February). The temporal variance and covariance quantities were partitioned into low pass ($\sim$ 10 - 90 days) and band pass ($\sim$ 2.5 - 6 days) components. The E-vector, as defined by Hoskins et. al. (1983), and quantities derived from it were the chief diagnostic tools.

The relationships of the transient effects near the exit region of the East Asian and North American (200 mb)jet maxima and their associated storm tracks are very similar to the schematic model presented by Hoskins (1983), but not for the North African jet maximum. The forcing from both the synoptic time scale and the low frequency eddies is basically equivalent barotropic, with the 200 mb and 700 mb patterns resembling each other.

For low frequency eddies, both the subtropical E-vector and the tropical transient kinetic energy indicate an equatorward energy propagation and a tropical response at 200 mb over the mid-Pacific where the zonal wind is westerly. However, the maxima of these two fields, which are longitudinally aligned, do not coincide with the maximum tropical westerlies. An analogous situation is not observed over the Atlantic.

The low frequency calculations reveal barotropic instability regions in the exit regions of the East Asian and North American jets and poleward of the NAJ maximum.

# I. INTRODUCTION

Since the publication of the work of Blackmon et. al. (1977) and Lau (1979 a,b) there has been a resurging interest in the time mean aspect of the three dimensional large scale atmospheric flow and variability therefrom. Blackmon et. al. (1977) presented data from the National Meteorological Center (NMC) operational analyses for 9 winters. The temporal variance and covariance quantities were partitioned into low pass ($\sim$ 10 - 90 days) and band pass ($\sim$ 2.5 - 6 days) components. They concluded that the jet streams in the time averaged flow develop as a result of thermally direct (time) mean meridional circulations over eastern Asia and North America, with thermally indirect circulations over the North Pacific and North Atlantic. Lau (1978) using a similar data set found that the transient eddy statistics are in good agreement with what would be expected for developing baroclinic waves. The distribution of eddy momentum flux is characterized by strong convergence of westerly momentum into the storm track axis.

Both of the above studies and Lau (1979a) have demonstrated that large longitudinal variations occur in the time mean and transient eddy quantities. The vertical structure and the transfer properties of the bandpass eddies in the storm track areas are typical of developing baroclinic waves whereas those of the low pass eddies in the regions of the maximum variance indicate a more equivalent barotropic behaviour. The transient eddy (TE) forcing, which is the largest in the upper troposphere, tends to shift the mean subtropical jet (STJ) polewards and aids in counterbalancing the effect of mean vorticity sources

and sinks due to surface friction. The main effect of the transient eddy momentum fluxes in the middle latitudes is to enhance the barotropic component of the time mean flow and to compensate for the effects of surface friction, Holopainen, Rontu and Lau (1982), Holopainen (1983), Holopainen (1978), Holopainen and Oort (1981a,b).

Recently, Hoskins (1983) and Hoskins et. al. (1983) introduced the concept of an extended Eliassen-Palm flux or E-vector as a diagnostic tool to study the transient/mean flow interactions. This vector (or more properly pseudovector) provides a measure of the effects of the transient forcing. The traditionally used meridional convergence of the zonal momentum flux, $\partial(u'v')/\partial y$, does not yield a complete description in the case of zonally varying mean flows. The E-vector contains information (within the limits of certain approximations) on the spatial orientation of of the eddies and the direction of their propagation. Diagnostic computations of this vector allow a two dimensional description of the effects of transient eddies on a horizontal map. Using this vector, Hoskins (1983, 1985), Hoskins et. al. (1983) and James (1983) have studied the transient/mean flow interactions in the midlatitudes.

Studies of the zonally asymmetric time mean circulation must address the maintenance of the subtropical jets and their interactions with the transient eddies and meridional circulations. However, the data coverage in the low latitudes is often sparse and numerical weather prediction (NWP) model forecasts are commonly used in the operational data assimilation. Partly because of these reasons previous studies, such as Blackmon et. al. (1977), have often excluded tropical regions equatorward of $20^{\circ}N$. Furthermore,

all previously published studies using the E-vector computations are limited to data of a single winter season. For studies using operational data sets produced by the National Meteorolgical Center (NMC) of more than a few years, the analysis system is not homogenous throughout the period.

In this study we will use the Numerical Variational Analysis (NVA) for the global tropics produced operationally by the U. S. Navy to study the time mean and transients of the winter circulations for a nine-year period, from 1974/75 to 1982/83. A climatology of the E-vector and quantities computed from it will be produced and used as the main diagnostic tools in Part I. For our purpose this data set has several advantages, including the absence of any NWP model forecast as a first guess, the retention of the analyzed divergence field which has proven useful in synoptic time variation studies over the tropical western Pacific, and the stable analysis scheme which has remained unchanged since 1974. The use of the tropical data allows us to look at the North African jet in addtion to the attention normally focused on the East Asian and North American jets. In addition, it will be possible to compute the equatorward energy propagation from the midlatitudes. These were previously studied mainly in theoretical or numerical models.

In this paper the data source and computation procedures are described in Section 2. Section 3 presents the nine-year means of the E-vectors and various quantities computed from it. The results are used to discuss the transient mean flow interaction and equatorward energy propagation. Section 4 presents the relations of the quantities in Section 3 to the storm track organization and low-level wind shear. Section 5 contains concluding remarks and a summary of the results.

## II. DATA SOURCES AND HANDLING

**A. FNOC Numerical Variational Analysis**

The wind data used in this work are the operational analyses of the Numerical Variational Analysis (NVA) produced by the U. S. Navy's Fleet Numerical Oceanography Center (FNOC). These data are produced four times daily by objective procedures on a mercator grid which extends from $40^{\circ}$S to $60^{\circ}$N. The use of the mercator secant projection results in a change in the actual distance between grid points from 140 km at $60^{\circ}$N to a maximum value of 280 km at the equator.

The winds are analyzed at the surface, 700, 400, 250 and 200 mb levels using a successive corrections technique based on the work of Cressman (1959). The first guess field is the six hour persistence field. These fields are then adjusted to be consistent with a set of numerical variational analysis equations which have incorporated the dynamical constraints of the momentum equations with friction included in the surface layer, (Lewis and Grayson, 1972). However, the surface and 200 mb wind data serve only as a lower and upper boundary condition for the NVA and are not subject to an adjustment.

An advantage of these data is that no model first guess is used which might bias the analysis in data sparse regions. The lack of a model providing a first guess is also a disadvantage since the analysis reverts to (6 hour) persistence when faced with a data void. Given the present state of tropical prediction this is not an altogether bad situation in the tropics but is considerably less satisfactory in midlatitudes. In any case this type of analysis cannot overestimate the transient activity. A small advantage of the Navy oper-

ational analyses is that some observations taken from ships are not transmitted on the GTS but are used in the analysis at FNOC. Another attractive feature of the data is the fact that the data analysis procedures have remained virtually unchanged since 1974. Thus the analyses are homogenous with respect to the objective analysis technique although the data base has changed as satellite observations have become more important and real time aircraft reports have become more numerous.

## III. COMPUTATIONS

Hoskins et. al. (1983) defines the E-vector as:

$$E = -\{ \, \overline{(u'^2 - v'^2)} \, , \, \overline{(u'v')} \, \} \quad (1)$$

where:

$( \;\; )' =$ deviation from seasonal mean

$\overline{( \;\; )} =$ seasonal mean.

It is important to note that as it stands the quantities used in the above definition are made up of transients with periods of 1 to 90 days. In this work a further decompostion of the transients into low and high frequency components is made using a low pass filter ( > 10 days ) and a band pass filter ( 2.5 to 6 days), respectively. Details of the filters and their response functions are given by Blackmon (1976).

Hoskins et. al. (1983) showed that where the E-vectors are divergent (convergent) there is a forcing of the mean circulation by the transients with a tendency to increase the westerly (easterly) mean flow. The E-vector also contains information relating to the orientation and direction of propagation of the eddies, (Hoskins et. al., 1983). A westerly (easterly) E-vector implies meridionally (zonally) elongated transient eddies with an eastward (westward) group velocity relative to the mean flow. The E-vector can be considered as an effective flux of easterly momentum or the horizontal component of an extended Eliassen-Palm flux. It follows that if we define a quantity $S_m$ such that:

$$\nabla^2(S_m) = -( \nabla \bullet E ) \quad (2),$$

then in the regions of $S_m$ maxima (minima) there is a tendency for westerly (easterly) acceleration of the mean flow by the eddies. This quantity rather than the actual divergence is presented, since as pointed out by Hoskins et. al. (1983) the E-vector divergence field is noisy and the noise obscures meaningful features. In the calculations the boundary at $60^{\circ}N$ does present a problem. This is a region of considerable eddy activity, and this boundary will have an adverse effect on the determination of $S_m$ The choice of zero as a northern and southern boundary when relaxing for $S_m$ appeared to give about as good a results as any.

Simmons et. al. (1983) showed that the local growth of the kinetic energy associated with deviations from the mean state is given by

$$\partial(KE')/\partial t = CK_x + CK_y$$

where

$$CK_x = -\frac{1}{a}\left(u'^2 - v'^2\right)\left\{\frac{1}{\cos(\theta)}\frac{\partial \bar{u}_b}{\partial \lambda} - \bar{v}_b \tan(\theta)\right\}$$

$$CK_y = -\frac{1}{a}\, u'v'\left\{\cos(\theta)\frac{\partial}{\partial \theta}\left(\frac{\bar{u}_b}{\cos(\theta)}\right) + \frac{1}{\cos(\theta)}\frac{\partial \bar{v}_b}{\partial \lambda}\right\}$$

where $\bar{u}_b$ and $\bar{v}_b$ are the components of the time mean wind, a is the radius of the earth, $\lambda$ is the longitude and $\theta$ is the latitude.

They further showed that

8

$$\partial(KE')/\partial t \sim \{ E \bullet \nabla u_b \}$$

where $u_b$ is the time mean zonal wind.

For convenience we define a notation such that:

$$S_E = \{ E \bullet \nabla u_b \} \qquad (3)$$

In regions where $S_E$ is positive (negative) there is a local growth (decay) of the eddies by interaction with the time mean flow.

The transient kinetic energy (TKE) was computed using the formula

$$TKE = ( u'^2 + v'^2 ) \qquad (4)$$

This quantity was computed for both the low and band pass transients as well as the unfiltered transients.

# IV. 200 MB MEAN FLOW / TRANSIENT INTERACTIONS

## A. E-vectors

Figure 1 presents the mean wintertime 200mb E-vector and zonal wind. In the zonal wind field we identify three jet maxima. These will be termed the East Asian jet (EAJ) centered at $135^\circ$E, $32^\circ$N, the North American jet (NAmJ) centered at $75^\circ$W, $35^\circ$N, and the North African jet (NAfJ) centered at $35^\circ$E, $27^\circ$N. It may be arguable whether the NAfJ should be treated as a separate jet maximum on a par with the EAJ and NAmJ or merely as an extended portion of the entrance region of the EAJ. The work of Krishnamurti (1961) clearly shows three distinct maxima, for the single winter that he examined. Arkin et. al. (1986) have a indication of a third maxima in their five-year average of NMC data. Chang and Lau (1980), also based on one season of data, showed that the daily variation of the NAfJ local jet maximum is often out of phase with the EAJ. Therefore the NAfJ may be considered as a separate entity from the EAJ. On the other hand, examination of individual winter means of the 200 mb wind indicates that in some years the NAfJ is rather ill defined compared to the EAJ and NAmJ.

James and Hoskins (1985) cite evidence that for the winter of 1980/81 the transient activity about the NAfJ is due to internal baroclinic instability. This is in contrast to the EAJ and NAmJ which are regions of boundary (Charney type) baroclinic instability. However, James and Hoskins indicate that the internal instability mechanism generates transients that are qualitatively similar with respect to the patterns of momentum and heat fluxes to those of the Charney mode. In the following we will attempt to point out similarities and differences of the NAfJ system with the other two jet maxima.

The E-vectors and transient activity in the Southern Hemisphere are not going to be looked at in any detail due to the small amount of data available in that region. This lack of data has an especially detrimental effect on the resolution of the transients when peristence is used as a first guess in the analysis system. This fact combined with the weakness of the summer circulation make any conclusions about the Southern Hemisphere transients rather circumspect.

Figure 1a is the zonal wind and the low-pass E-vector. As was shown by Hoskins et. al. (1983) for the 1979/80 winter, the low-pass transients generally have a westward pointing E-vector .Hoskins et. al. (1983) present the 25C ab fields, but we feel that the comparison is valid. This is especially true in the exit regions of the East Asian and North American jet maxima and weakly so for the North African system. This implies that these transients are for the most part zonally elongated ($u'^2 > v'^2$) and westward propagating with respect to the mean flow. The NAmJ and NAfJ are similar in the entrance regions with weak northerly E-vectors which implies that $v'^2 \sim u'^2$ . Figure 1a may also be compared to the E-vectors computed by Simmons et. al. (1983) (their Fig. 16) for the fastest growing mode of their barotropic model linearized about a climatological mean 300 mb flow. Since the period of this mode is approximately fifty days, it may be considered a low pass mode. The two fields are similar in the exit regions of the EAJ and NAmJ jets where both show large E-vector magnitudes. However, Figure 1a shows large E-vectors south of the NAmJ which are absent in Simmons' et. al. (1983) mode and Figure 1a does not have the large magnitudes in the Bering Sea region shown by Simmons et. al. (1983).

Opposite to the low-pass E-vectors, the band-pass E-vectors ( Figure 1b) tend to point eastward. This implies that the band pass eddies are for the most part meridionally elongated($v'^2 > u'^2$) and eastward propagating with respect to the mean flow. There are maximum values in the exit regions of the EAJ and NAmJ.

Figure 1c is a plot of the unfiltered E-vectors. The direction is predominantly equatorward across the jet latitudes. There is a tendency for the low-pass signal to dominate in the EAJ region and for the band-pass to dominate in the NAmJ region. The NAmJ and NAfJ are alike in that they have strong northerly E-vectors in the entrance regions. In this instance, the NAfJ looks as if it is the entrance region for a combined NAfJ - EAJ system. If one takes such a view, the combined system resembles the NAmJ structure with respect to the orientation of the E-vectors in the entrance and exit regions.

The Southern Hemisphere has the reduced transient activity during the summer season. In addition, the poor data coverage together with the use of persistence as a first guess undoubtedly underestimates the eddy activity there. Nonetheless, in Figure 1a one can still see the general westward pointing low pass E vectors, and in both Figure 1a and c, the tendency of an equatorward direction. The band pass vectors, Figure 1b, are too small to make any definite conclusions.

The E-vectors at 700 mb (not shown) are similar in orientation and relative magnitude to those at 200 mb. This is most pronounced over the northern portions of the northern hemisphere ocean basins in the exit regions of the EAJ and NAmJ. The pattern at 700 mb in the NAfJ region is rather nondescript

12

The similarity of the 700 mb and 200 mb fields suggests that the 200 mb fields give a good representation of the vertically integrated E-vector structure for the northern midlatitudes.

## B. Transient kinetic energy

Figure 2 presents plots of the low-pass, band-pass, and unfiltered transient kinetic energy (TKE),as defined by (4), at 200mb. The gross pattern of the unfiltered field (Figure 2c) resmbles those computed by Murakami and Unninayar (1977, Fig. 3 ) for the winter of 1970-71 and Arkin and Webster (1985, Fig. 3a) for the average of 1968-79 winters, both based on NMC data. With the exception of the NAfJ which has a TKE maximum along its poleward flank, the exit regions of the jet maxima are clearly regions of enhanced eddy activity. This could be anticipated from the magnitudes of the E-vectors in Figure 1. For all plots the TKE maximum tend to be at about the same latitude of the jet maximum with a tendency for a poleward extension. This is consistent with the single season results of Hoskins et. al. (1983), Hoskins (1985) and James (1983). James and Hoskins (1985) noted a maximum of high frequency TKE on the poleward flank of the NAfJ between 400 and 200 mb for the winter of 1980/81. They attributed this maximum to internal baroclinic instability.

The model results of Simmons et. al. (1983) consistently point to a low pass TKE maximum in the eastern Pacific, and a secondary maximum in the Atlantic. Both maxima are in the regions of the exit of the jets but farther poleward than the maxima of Figure 2a.

13

The low pass and unfiltered TKE (Figure 2a and Figure 2c) display zones of maximum values across the Tropics centered at $160^\circ$W and around $30^\circ$E. This tropical penetration was also noted by Murakami and Unninayar (1977). These are both regions of westerlies at 200mb (see Figure 1). Arkin and Webster (1985) documented the fact that the equatorial westerlies are a favored region of enhanced TKE. This is consistent with the theory of Webster and Holton (1982) which predicted that waves from the mid-latitudes could penetrate into the tropics through ducts formed by tropical westerlies. Webster and Holton (1982) showed that the observed variance due to low pass transients exhibit maxima in the region of time mean westerlies.

Figure 3 contains plots of low pass TKE, E-vectors and zonal wind for the band $20^\circ$N to $20^\circ$S over the central Pacific. Since the magnitudes of the E-vectors and TKE are generally much smaller in the tropics a separate plot of this region is needed to see the details in this region. It also may be used to represent the unfiltered pattern because the band pass E-vectors are generally much smaller than the low pass in this region in both hemispheres. What is apparent in Figure 3 is the strong equatorward E-vector in the central Pacific. While this flux of energy from higher latitudes is coincident with the regions where the wind is westerly, the maximum is not in the region of the strongest westerlies. This result is different from that of Arkin and Webster (1985), who indicated that the largest TKE values are associated with the strongest westerly winds. In Figure 3 the maximum flux from the northern hemisphere is located near 153W - 160W, which is just to the east of the exit region of the EAJ. The maximum westerlies along

14

15N is, on the other hand, near 130W. Consistent with the maximum E-vectors, the maximum TKE at the equator is near 160W. This is a region of westerlies, but again not the strongest westerlies whose equatorial location is near 125W.

The results shown in Figure 3 compare favorably with the modeling work by Hendon and Hartmann (1985) and Hendon (1986). Hendon and Hartmann (1985) showed that the maximum variance in regions of westerlies in the tropics is due to enhanced equatorward propagation of low pass transients. Hendon's (1986) model has only a fairly uniform easterly flow between 10N and 10S, and the only forcing is topo-graphic. However, this forcing resembles the Tibetan Plateau, therefore the midlatitude and subtropical results produced by his model may be considered relevant when compared with the EAJ circulation. His model displays strong northerly E-vectors across 20N, just to the east of the exit region of the jet maxi-mum at 30N. As in Figure 3 his E-vectors then turn and become easterly west of 155W and westerly to the east of this longitude.

One possibility that comes to mind in considering Figure 3 is that the tropical transient activity in the regions of the tropical westerlies is being driven by transients propagating from the midlatitudes. This is probably the case in Hendon's model since it had no convective parameterization. In such a case one could sketch out the following relations. The increased(decreased) midlatitude transient activity produces stronger(weaker) fluxes ($E_y$ < 0) equatorward. In regions where the the zonal tropical wind is westerly then more(less) energy propagates into the Tropics producing larger(smaller) values of TKE. Figure 4a

15

and Figure 4b are time longitude plots of the seasonally averaged 200 mb unfiltered TKE averaged from $10^{\circ}N$ to $10^{\circ}S$, and the 200 mb $E_y(= u'v')$ at $15^{\circ}N$, respectively. There appears to be evidence for the association of enhanced tropical TKE and increased northerly E-vector at $160^{\circ}W$. Of course the sample size of nine-years renders to speculation how well the atmosphere actually follows the above relation. The sources of tropical variability are not driven solely by transients propagating from the northern hemisphere. In order to evaluate more definitely the amount of tropical variance being forced by midlatitude flow a longer time series would be needed so that signal and noise can be separated.

It is not clear that the same type of midlatitude - tropical interaction is taking place in the exit region of the NAmJ near $30^{\circ}W$. Figure 5 shows the low-pass TKE, E-vectors and zonal wind for the tropical Atlantic. There is a strong equatorward E-component along the eastern coast of Brazil and a large TKE maximum accompanying it. There are northerly E-vectors across the tropical north Atlantic and a TKE extrusion along the North Africa coast, coincident with a region of strong westerlies. In any case the pattern is not nearly as suggestive of an equatorward propagation of transients from the northern midlatitudes as was seen in the Pacific, although there is again a strong indication of a flux from the Southern Hemisphere.

The difference from the North Pacific pattern is probably a result of the structure of the NAmJ. The NAmJ has a northeast-southwest tilt while the EAJ axis is east-west oriented. Thus the exit region of the NAmJ and the associated TKE activity are farther north.

## C. Eddy momentum flux

Simmons et. al. (1983) relates the convergent/divergent patterns of the low pass E-vectors to the sources of low frequency barotropic instability. They interpreted strong divergence as an indication of a source region of low frequency eddies observed in their model simulations. Figure 6 is a plot of $S_m$ { $=$ $\nabla^{-2}(-\nabla \bullet E)$ } at 200mb. Maxima (minima) of this quantity can be considered as centers of westward (eastward) momentum flux convergence due to the actions of the transient eddies. Maxima are regions where the transients tend to make the time mean flow more westerly. For the EAJ and the NAmJ the effect of the low pass eddies (Figure 6a) is a tendency to decrease the strength of the jet maxima and to move the maxima eastward of their observed position. The transient forcing is very weak about the NAfJ, however the entrance regions of the NAfJ and the NAmJ look similar.

The centers of the band pass $S_m$, Figure 6b, are somewhat farther west from the low pass centers for the EAJ and NAmJ. They have a tendency to move the jet cores to the north northeast and to decelerate the flow in the jet entrance regions. The band pass $S_m$ fields are more zonally elongated and are maximum along the poleward side of the jets, therefore they have a tendency to decrease the cyclonic shear of the jetstream. The NAfJ pattern is again very weak, but appears to be qualitatively similar to the other two jet maxima.

The unfiltered $S_m$ field, Figure 6c, has positive values which extend across both northern hemisphere ocean basins. There is a tendency for the EAJ and the NAmJ to have a negative entrance region and a

17

positive exit region. This result is consistent with that of Blackmon et. al. (1977). The NAfJ, on the other hand, is more or less surrounded by negative values.

Hoskins (1983), using scaling analysis, argued that the barotropic forcing should be dominant in the jet exit regions. This is borne out in Figure 7 which shows the unfiltered 700 mb $S_m$ field. Here the maxima coincide with those at 200 mb in the exit regions of the EAJ and NAmJ.

Many studies of the effects of eddies on the mean flow used the zonally averaged poleward momentum flux ( $u'v'$ ) only. As shown in Section 3, this is the meridional component of the E-vector which goes into the computation of $S_m$. We can perform a calculation analogous to $S_m$ but just using the ( $u'v'$ ) component of the E-vector. Denoting the result by the notation $S_{my}$, we have

$$\nabla^2( S_{my} ) = \partial(-u'v')_i\partial y. \quad (5)$$

This would produce fields in which the relative maxima indicate the momentum flux convergence due to the meridional variations of the ($u'v'$) correlation. The zonal average of the $S_m$ and $S_{my}$ computations would be equal. Figure 8 shows the low pass $S_{my}$ at 200 mb. Compared to the $S_m$ shown in Figure 6a the $S_{my}$ maxima in the Pacific are shifted towards North America and generally have somewhat less zonal structure than the corresponding $\dot{S}_m$ fields. As reported by Hoskins et. al. (1983), the zonal scale of the $u'v'$ correlation is larger than the meridional scale. The zonal variation of $u'^2 - v'^2$ becomes largest in regions of strong westerlies, leading to large differences between $S_{my}$ and $S_m$ in these regions. Although the band pass $S_{my}$ field (not shown) more closely resembles that for $S_m$, evidently because of less varia-

18

tion of $u'^2 - v'^2$ in the zonal direction, the unfiltered $S_{my}$ (not shown) with a rather bland zonal structure is quite different from the unfiltered $S_m$( Figure 6c). These differences point out the importance of zonal variations, which cannot be represented by $u'v'$, in considering the local momentum balance. The $u'^2 - v'^2$ term is especially important in determining the local eddy vorticity flux convergence. It has been shown in Figure 1b that the synoptic-scale transient eddies tend to be elongated in the meridional direction (westerly E-vectors). If one is interested in parameterizing the effects of these eddies, a representation of the time average of the $u'^2 - v'^2$ term would be more appropriate than the much discussed $u'v'$.

Another way to examine the transient forcing of the mean flow is to look at the vorticity balance. The time averaged vorticity equations can be written approximately as (Hoskins et. al., 1983)

$$\partial \zeta / \partial t + V \bullet \nabla \zeta + f \nabla \bullet V + \nabla \bullet (V' \zeta') = k \bullet \nabla x \, F,$$

where f is the Coriolis parameter, and F is the frictional force.

Taking the vertical integral (denoted by square brackets) through the depth of the troposphere yields

$$\left[ \partial \zeta / \partial t \right] + \left[ V \bullet \nabla \zeta \right] + \left[ \nabla \bullet (V' \zeta') \right] \sim \left[ k \bullet \nabla x \, F \right]$$

Additionally, Hoskins et. al. (1983) show, that to a good degree of approximation:

$$\nabla \bullet (V' \zeta') \sim \partial (\nabla \bullet E) / \partial y. \qquad (6)$$

Figure 9 are the low pass, band pass and unfiltered fields at 200 mb of $-\nabla^{-2} \partial (\nabla \bullet E) / \partial y$. The correspondence of the low pass and band pass fields with those of Fig. 5 of Hoskins et. al. (1983) is quite good, considering that they were looking at only a single winter.

The low pass transient forcing is in general greater than that of the band pass. The "quadrapole" structure observed in the mid-Pacific by Hoskins et. al. (1983) is also apparent in Figure 9a and weakly discernable in the Atlantic. The vorticity flux convergence is negatively correlated with the mean vorticity, indicating that the low pass transients tend to smooth out the time mean (stationary) long waves. The band pass forcing Figure 9b, is also similar to that of Hoskins et. al. in that anticyclonic (cyclonic) forcing is found equatorward (poleward) of the storm tracks in both northern hemisphere ocean basins. However, Hoskins et. al. (1983) found that the band pass vorticity flux forcing is strong only in the Atlantic, while Figure 9b, indicates that it is also important in the Pacific. Hoskins et. al. (1983) note that the year they considered was one of anomalously decreased transient activity along the Pacific storm track.

Hoskins (1983) developed a scaling model for the synoptic transient forcing, in which the vorticity flux convergence has a dipole structure that saddles the northern flank of the jet exit regions. The result is a tendency for the eddies to move the jet maximum downstream and polewards in the exit region and to split the westerly flow at the diffluent end of the jet. The band pass eddy vorticity flux convergence patterns ( Figure 9b) for the EAJ and NAmJ are consistent with Hoskin's model, but not at all for the NAfJ where the net tendency is to move the jet core equatorward. This difference from Hoskin's model is apparently due to the smaller zonal extent and, perhaps to a lesser degree, the lower latitude of the NAfJ.

Figure 10 is the mean surface streamfunction computed from the nine year mean surface wind components using the method described in Chang and Lau (1982). Since the vorticity is related to the Lapla-

20

cian of this quantity, it is consistent to think of minima (cyclones) to be sinks of vorticity due to frictional processes at the surface and maxima (anticyclones) to be source regions. What is striking is that the eddy convergence of vorticity at 200 mb (Figure 9b) is coincident with the surface centers of cyclonic circulation. This would be expected if the upper tropospheric contribution to the eddy fluxes is the dominant term in the vertically averaged, time mean vorticity equation and the the eddy fluxes dominate the vertically averaged advection. As was shown by Holopainen and Oort (1981b), the balance struck over the North Pacific Low is

$$\nabla \cdot \overline{V'\zeta'} \ \sim \ -g \, k \cdot \overline{\nabla \times \tau}_s,$$

where $\tau_s$ is the surface stress. Holopainen and Oort (1981a,b) show that the vertical integral of the eddy vorticity flux convergence plays a major role in balancing the surface stress since the advection term tends to cancel in the vertical. The synoptic transient eddies act to maintain the surface cyclonic flow to the north and anticyclonic flow to the south and east of the storm track. Thus our result verifies the result of Holopainen and Oort (1981b) for an independent data set, and also gives a boost in the confidence in the transient eddy computations at 200 mb over the Northern Hemisphere oceanic regions.

D. Barotropic instability ($S_E$)

Simmons et. al. (1983) integrated a global barotropic model, which is linearized about a climatological January 300 mb flow and perturbed by a series of localized forcings in the tropics and subtropics. They used a quantity similar to

$$S_E = (\overline{E} \cdot \nabla \overline{u}),$$

21

which represents the local conversion of kinetic energy from the mean flow to transient eddies, as a measure of barotropic instability. On the basis of their results and the work of Hoskins et. al. (1983), they suggest that much of the low frequency variability of the Northern Hemisphere wintertime general circulation is associated with disturbances which derive their energy from the time mean basic state through barotropic instability. Figure 11 is a plot of $S_E$ for the low pass, band pass and unfiltered data. As noted by Simmons et. al. (1983), some caution is needed in interpreting positive values of the conversions as indications of barotropic instability. This interpretation is strictly valid only for the global integral. The local contribution to the conversion terms do not directly yield local growth of eddy energy because of the existence of additional flux terms which distribute the energy while contributing nothing to the global mean values. Figure 11a, the low pass $S_E$, is analogous to Fig. 17 of Simmons et. al. (1983). However, important differences are found, which may be expected since the simple structure shown by Simmons et. al. is that of a single, most unstable mode. In Figure 11a the large values of $S_E$ in Simmons et. al.'s Bering Sea region and the North Atlantic near 60N are missing. Instead, the large positive values are concentrated in the belt of 30 - 40N, including the exit regions of the EAJ and NAmJ, and a zone across North Africa. Figure 11a also shows that both the EAJ and the NAmJ have weak negative values in the entrance regions. The NAfJ, on the other hand, has a negative $S_E$ in the jet itself. These structures suggest that the low pass eddies are barotropically generated or maintained in the exit regions of the major jets, and north of the NAfJ along 30N.

22

The band pass $S_E$, Figure 11b, values are generally smaller than the low pass. This is not surprising as the band pass eddies are known to draw energy from baroclinic instability. In the NAfJ region the band pass and low pass fields look similar. On the other hand, the two fields look different elsewhere. Positive values are observed in the entrance region of the EAJ and in a zonal belt along 40N from the jet maximum to the exit region. There is no evidence of a secondary positive maximum to the south of the jet axis as seen in the model integrations of Hendon (1986). Around the NAmJ, the band pass $S_E$ structure is completely reversed from that of the low pass, with North America being a source of kinetic energy for the band pass transients and the Atlantic a sink. The unfiltered $S_E$, Figure 11c, reflects the different nature of the low and band pass values about the EAJ and the NAmJ, resulting in small values over eastern Asia, the eastern Pacific and most of the Atlantic.

The different $S_E$ patterns around the three jets, especially those of the band pass eddies, suggest that the barotropic instability properties of the three jets are quite different from each other.

## V. STORM TRACKS AND UPPER-LEVEL JETS

### A. Storm tracks

Figure 12 presents plots of the surface transient kinetic energy for the low pass, band pass and unfiltered wind. The maxima are taken to be the principal storm tracks. The band pass TKE maxima in Figure 12b have the familiar storm track pattern seen in the data of Blackmon et. al. (1977) and Lau

23

(1979a,b). It should be noted that Blackmon et. al. (1977) and Lau (1979a,b) use maxima in the field of 1000 mb geopotential variance to define the storm tracks. They occur on the western side of the northern hemisphere ocean basins with a southwest to northeast tilt. For both the EAJ and the NAmJ, the band pass maximum at the surface is poleward and downstream of the 200 mb jet maximum. However, there is a difference between eastern Asia and eastern North America. The TKE contours cut westward deeply into the North American continent from the maxima in the Atlantic, but they parallel the Asian coast and make the Asian continent relatively storm free.

The low pass TKE (Figure 12a) in the Pacific has a maxima to the northeast of the band pass maximum. This could be explained by the slowing of the storms as they mature and deepen and finally stagnate in the eastern side of the Pacific, forming the Aleutian low. The corresponding feature in the Atlantic, the Icelandic Low, is off our charts. In the western Atlantic the low pass maxima is almost due north of the band pass maximum, this is a common position for storms to stagnate after they have deepend quite rapidly while moving northward. The Mediterranean region shows low pass transient activity but is quite nondescript in the band pass fields of TKE.

The unfiltered TKE field (Figure 12c) shows the concentration of activity in the northern part of the northern hemisphere ocean basins quite vividly.

The 700 mb TKE fields (not shown) in general resemble those at the surface. More activity is observed in the region of the NAfJ than at the surface. This perhaps in an indication that internal baro-

clinic instability may be more important in this region, James and Hoskins (1985). At both levels, there is little evidence of any equatorial penetration of TKE in the western Pacific, as was reported by Murakami and Unninayer (1977) in their calculation of the 700 mb TKE for the 1970-71 winter.

**B. Low-level wind shear**

Figure 13 is a plot of the magnitude of the low-level (surface to 700 mb) wind shear. To the extent that the thermal wind approximation is valid, this is related to the mean low-level thermal gradient. As expected, the largest values are found along and to the east of the Asian and North American continents beneath the 200 mb wind maxima. There are also large values across the northern African continent. In the Southern Hemisphere ( summer ) the strongest gradients tend to be on the west coasts of the continents, evidently related to the very cool waters off these coasts. The positions of the strong shear in the western ocean basins is consistent with the interpretation of the band pass TKE maxima in these regions as being the result of the growth of baroclinic waves.

## VI. SUMMARY AND CONCLUSIONS.

Based on the 1974-1983 FNOC global band analysis, a diagnostic study of the effect of transient eddies on the winter mean flow was carried out by E-vector and related computations. Our main results may be summarized as follows:

1. The forcing from both the synoptic time scale and the low frequency eddies is basically equivalent barotropic, with the 200 mb and 700 mb patterns resembling each other.

2. The exit regions of the NAmJ and EAJ are quite similar in structure with respect to many of the features due to transients. The entrance region of the NAfJ resembles that of the NAmJ, but not the EAJ. In this regard the NAfJ may be considered as the entrance region of the combined EAJ/NAfJ system.

3. The maximum westerly forcing for all transients is on the western end of the storm track to the northeast of the major jet (EAJ and NAmJ) maxima at 200 mb. While all transient effects are a maximum in the exit regions, the synoptic time scale eddies have a more meridional orientation while the low frequency eddies are zonally elongated. The difference in shapes and the results of the eddy momentum flux convergence indicate that just considering the $\overline{u'v'}$ correlation will give an incorrect picture of the local momentum balance, and that the consideration of the $\overline{u'^2 - v'^2}$ term is of vital importance.

4. The relationships of the transient effects near the exit region of the major jets and storm tracks are very similar to the schematic model presented by Hoskins (1983), but not for the NAfJ.

5. The eddy vorticity forcing at 200 mb dominates the vertically integrated vorticity budget. This is consistent with the finding of Holopainen and Oort (1983) which suggests that the

26

surface mean circulations are maintained against frictional dissipation by upper level eddy fluxes.

6.  For low frequency eddies, both the subtropical E-vector and the tropical transient kinetic energy indicate an equatorward energy propagation and a tropical response at 200 mb over the mid-Pacific where the zonal wind is westerly. However, the maxima of these two fields, which are longitudinally aligned, do not coincide with the maximum tropical westerlies. An analogous situation is not observed over the Atlantic.

7.  The low frequency calculations reveal barotropic instability regions in the exit regions of the EAJ and NAmJ, and poleward of the NAfJ maximum. This instability distribution agrees with Simmons et. al. (1983)'s modeling result in the EAJ, but differs from their results considerably elsewhere.

8.  Comparison of the transient kinetic energy fields at the surface indicate the expected transition of a synoptic time scale maximum on the western side of the ocean basins to a low frequency maximum on the eastern side and farther north. This is consistent with life cycle of baroclinic waves developing on the western side and moving north-eastward while deepening and slowing down. The low frequency transient fields also tend to have an equivalent barotropic structure over the eastern ocean basins. This is apparently due to the vertical development accompanied by deepening, (Hoskins, 1983). What is apparent is that the

band pass surface TKE is most active in the left exit region of the jet which is to the north of the maximum in the low level baroclinicity. The transients have little effect on the acceleration of the jet maximum and appear in some regions to have a decelerating effect.

# REFERENCES

Arkin, P. A., V. E. Konsky, J. E. Janowiak, and E. A. O'Lenic, 1986: *Atlas of the tropical and sub-tropical circulation derived from National Meteorological Center Operational Analyses*, NOAA Atlas No. 7, Silver Spring , MD 8pp. (Copies can be obtained from: Climate Analysis Center. 5200 Auth Road, Washington D. C. 20233)

Arkin, P. A. and P. J. Webster, 1985: Annual and interannual variability of tropical-extratropical interaction: An empirical study. *Mon. Wea. Rev.*, 113, 1510-1523.

Blackmon, M. L., 1976: A climatological spectral study of the 500 mb geopotential height of the Northern Hemisphere. *J. Atmos. Sci.*, 33, 1607-1623.

Blackmon, M. L., J. M. Wallace, N.-C. Lau and S. L. Mullen, 1977: An observational study of the Northern Hemisphere wintertime circulation. *J. Atmos. Sci.*, 34, 1040-1053.

Chang, C.-P., and K. M. Lau, 1980: Northeasterly cold surges and near-equatorial disturbances over the winter MONEX area during December 1974. Part II: Planetary scale aspects. *Mon. Wea. Rev.*, 108, 298-312.

Chang, C.-P., and K. M. Lau, 1982: Short-term planetary-scale interactions over the tropics and midlatitudes during Northern winter. Part I: Contrasts between active and inactive periods. *Mon. Wea. Rev.*, 110, 933-946.

Cressman, G. P., 1959: An operational objective analysis system. *Mon. Wea. Rev.*, 87, 367-374.

Hendon, H. H., 1986: Time-mean flow and variability in a nonlinear model of the atmosphere with orographic forcing. *J. Atmos. Sci.*, **43**, 433-448.

Hendon, H. H., and D. L. Hartmann 1985: Variability in a nonlinear model of the atmosphere with zonally symmetric forcing. *J. Atmos. Sci.*, **42**, 2783-2797.

Holopainen, E. O., 1978: On the dynamic forcing of the long term mean flows by the large scale Reynold's stresses in the atmosphere. *J. Atmos. Sci.*, **35**, 1596-1604.

Holopainen, E. O., 1983: Transient eddies in mid-latitudes: observations and interpretation. *Large-Scale Dynamical Processes in the Atmosphere,*, B. Hoskins and R. Pearce, Eds., Academic Press. 397pp.

Holopainen, E. O. and A. H. Oort, 1981a: Mean surface stress curl over the oceans as determined from the vorticity budget of the atmosphere. *J. Atmos. Sci.*, **38**, 262-269.

Holopainen, E. O. and A. H. Oort, 1981b: On the role of large-scale transient eddies in the maintenance of the vorticity and enstrophy of the time mean atmospheric flow. *J. Atmos. Sci.*, **38**, 270-280.

Holopainen, E. O., L. Rontu and N.-C. Lau, 1982: The effect of large-scale transient eddies on the time mean flow in the atmosphere. *J. Atmos. Sci.*, **39**, 1972-1984.

Hoskins, B. J., 1983: Modelling of the transient eddies and their feedback on the mean flow. *Large-Scale Dynamical Processes in the Atmosphere,*, B. Hoskins and R. Pearce, Eds., Academic Press, 397pp.

Hoskins, B. J., 1985: The middle latitude transients in the FGGE year and their role in the seasonal mean momentum and heat budgets. *Report of the seminar on progress in diagnostic studies of the global atmospheric circulation as a result of the global weather experiment, Helsinki, August 1984*, GARP Special Report No. 42, WMO, Geneva, Switzerland.

Hoskins, B. J., I. N. James, G. H. White, 1983: The shape, propagation and mean-flow interaction of large scale weather systems. *J. Atmos. Sci.*, **40**, 1595-1612.

James, I. N., 1983: Some aspects of the global-circulation of the atmosphere in January and July 1980. *Large-Scale Dynamical Processes in the Atmosphere,*, B. Hoskins and R. Pearce, Eds., Academic Press, 397pp.

James, I. N.and B. J. Hoskins, 1985: Some comparisons of atmospheric internal and boundary baroclinic instability. *J. Atmos. Sci.*, **42**, 2142-2155.

Krishnamurti, T. N., 1961: The subtropical jet stream of winter. *J. Meteor.*, **18**, 172-191.

Lau, N.-C., 1978: On the three-dimensional structure of the observed transient eddy statistics of the northern hemisphere wintertime circulation. *J. Atmos. Sci.*, **35**, 1900-1923.

Lau, N.-C., 1979a: The structure and energetics of transient disturbances in the Northern Hemisphere wintertime circulation. *J. Atmos. Sci.*, **36**, 982-995.

Lau, N.-C., 1979b: The observed structure of tropospheric stationary waves and the local balances of vorticity and heat. *J. Atmos. Sci.*, **36**, 996-1016.

Lewis, J. M. and T. H. Grayson, 1972: The adjustment of surface wind and pressure by Sasaki's variational matching technique. *J. Appl. Meteor.*,11, 586-597.

Murakami, T. and M. S. Unninayar, 1977: Atmospheric circulation during December 1970 through February 1971. *Mon. Wea. Rev.*, 105, 1024-1038.

Simmons, A. J., J. M. Wallace, and G. W. Branstator, 1983: Barotropic wave propagation and instability, and atmospheric teleconnection patterns. *J. Atmos. Sci.*, 40, 1363-1392.

Webster, P. J. and J. R. Holton, 1982: Cross-equatorial response to middle-latitude forcing in a zonally varying basic state. *J. Atmos. Sci.*, 39, 722-733.
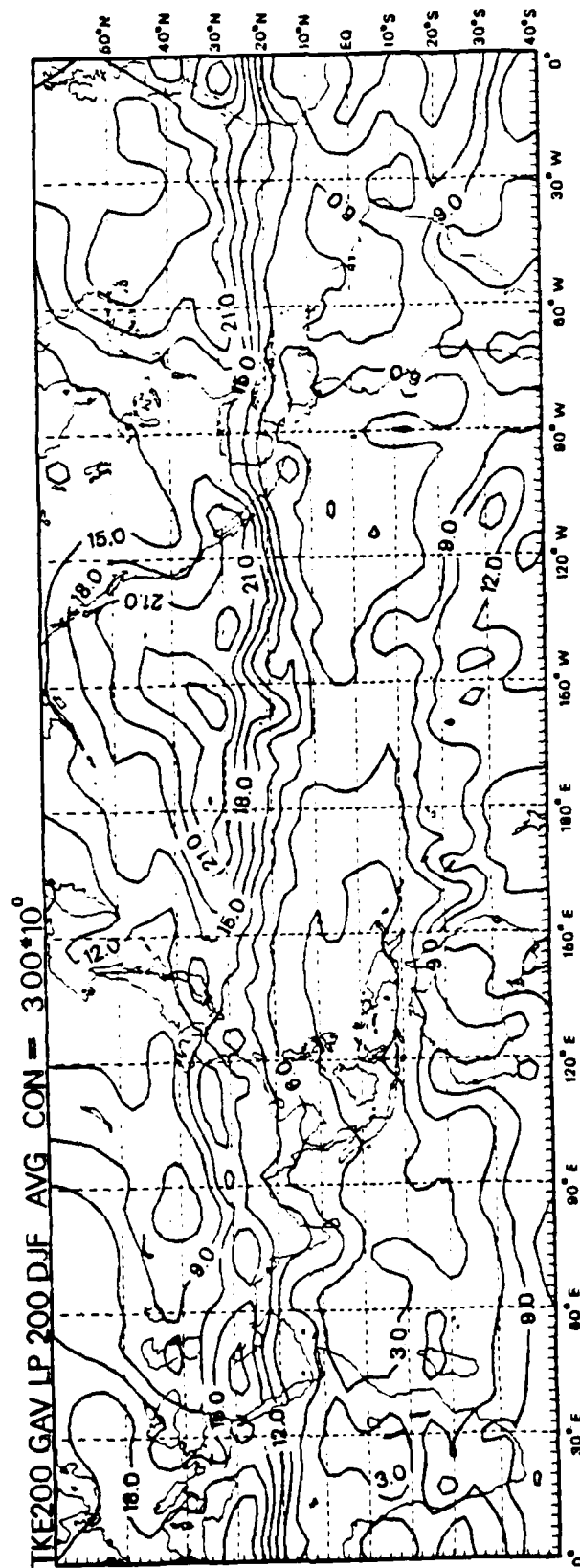
Fig. 1A

33

E + U GAV BP 200 DJF AVG CON = 1.00*10¹     SCALE = 5.000*10⁰

Fig. 1B

34

E + U GAV UN 200 DJF AVG CON = 100*10¹

SCALE = 1000*10¹

Fig. 1C

35

TKE200 GAV LP 200 DJF AVG CON = 3.00*10⁰

Fig. 2A

36

TKE200 GAV BP 200 DJF AVG CON = 150*10⁰

Fig. 2B
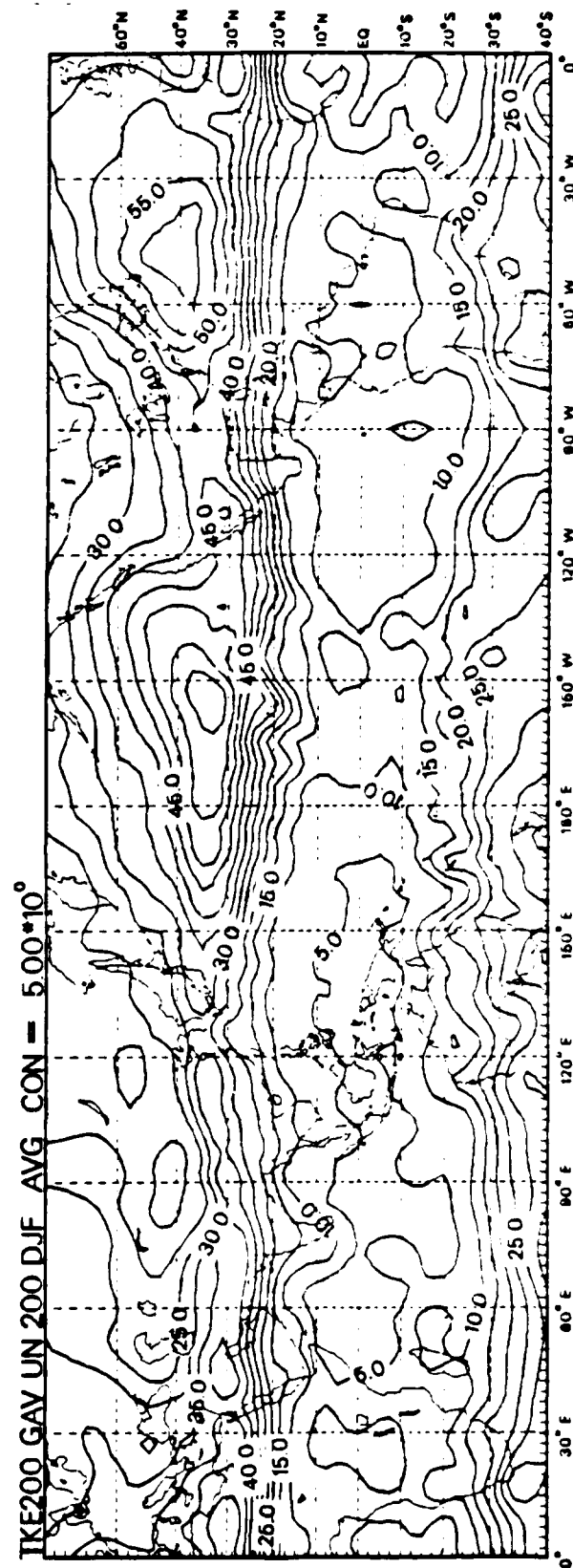
TKE200 GAV UN 200 DJF AVG CON = 5.00*10⁰

Fig. 2C

38

Fig. 3B

Fig. 3A
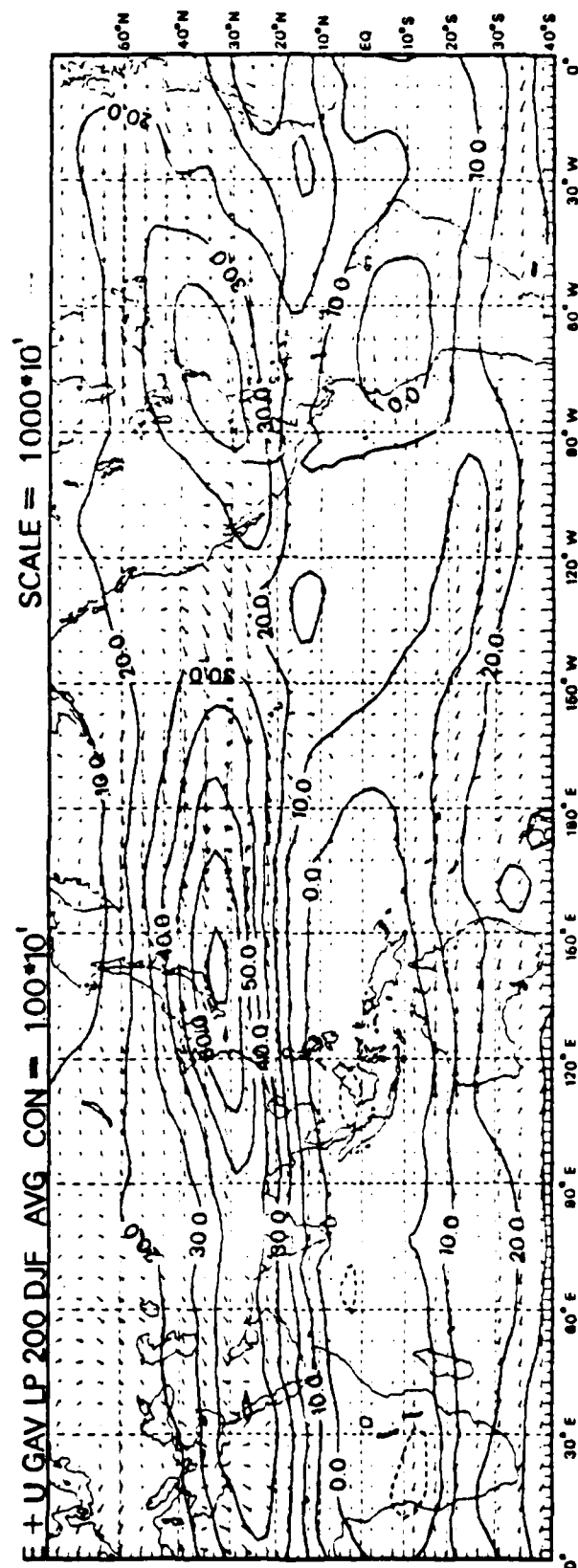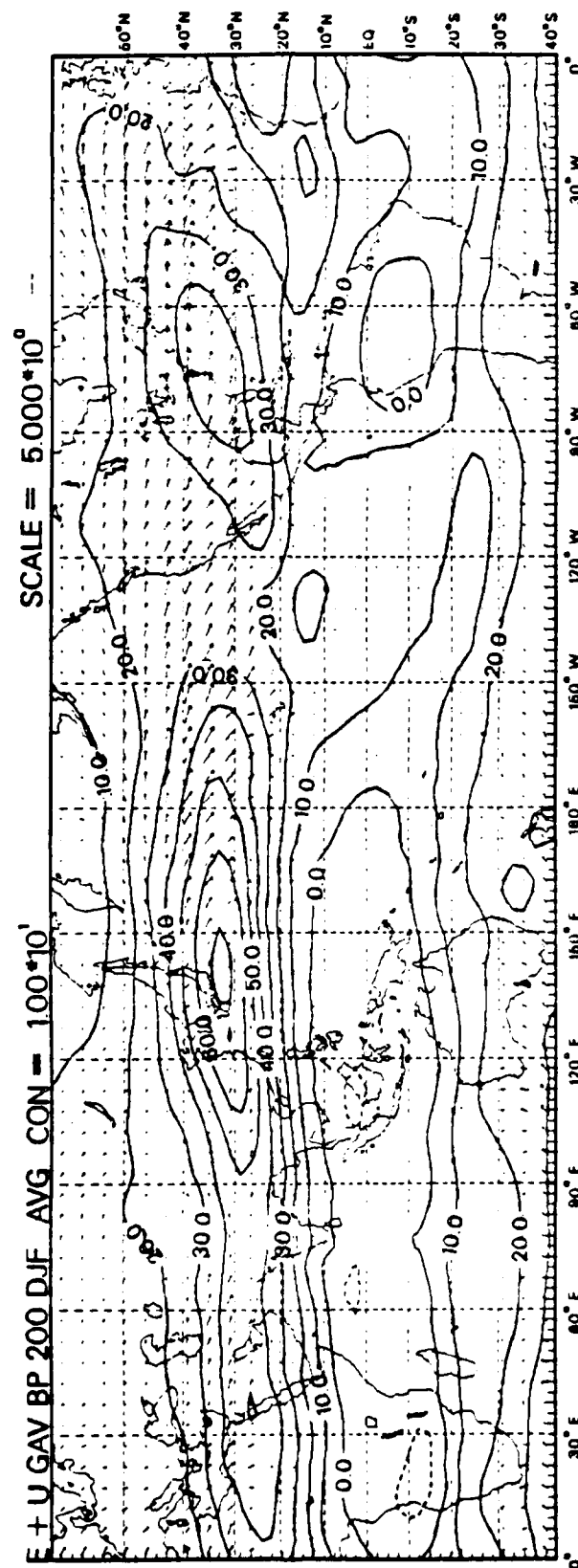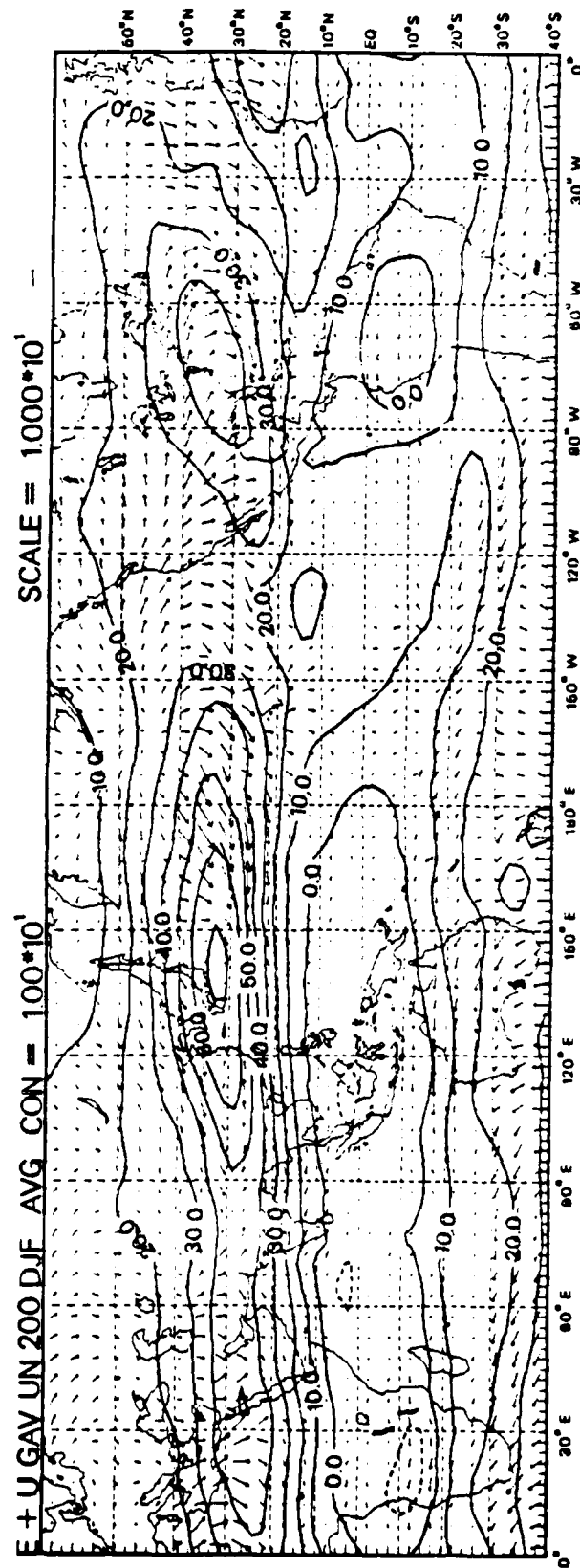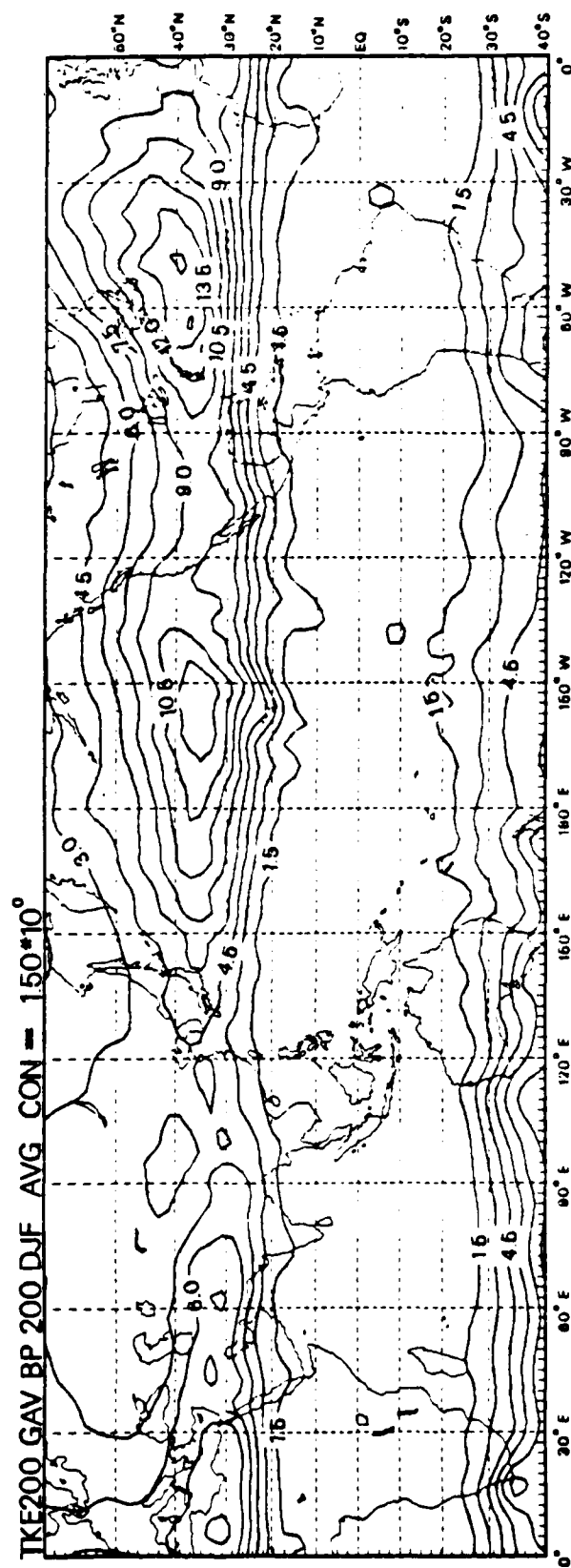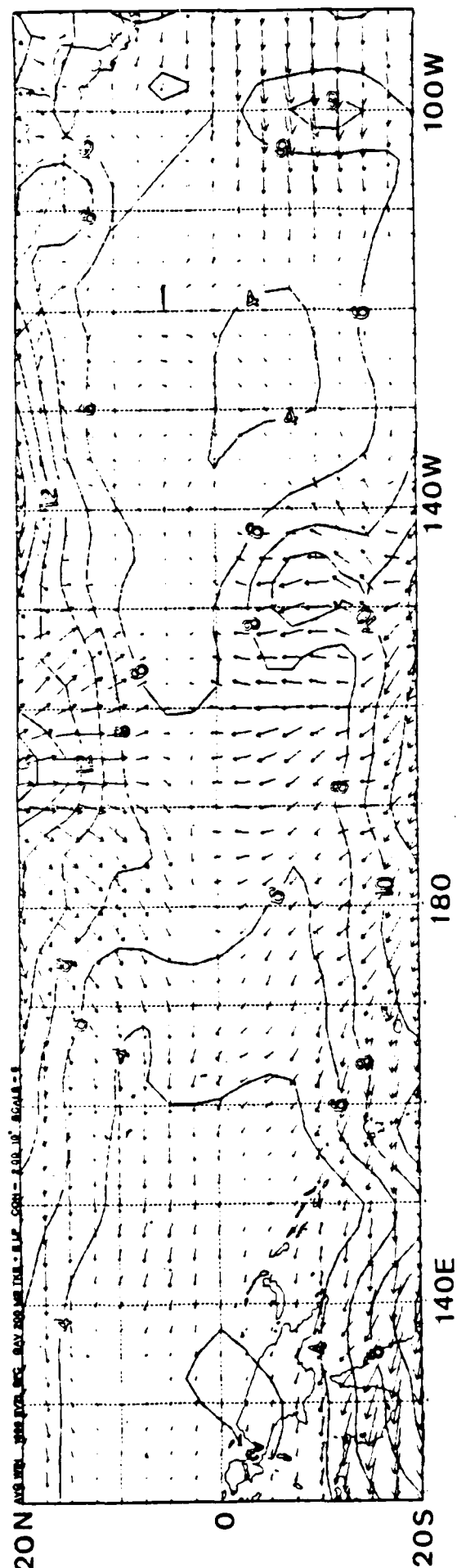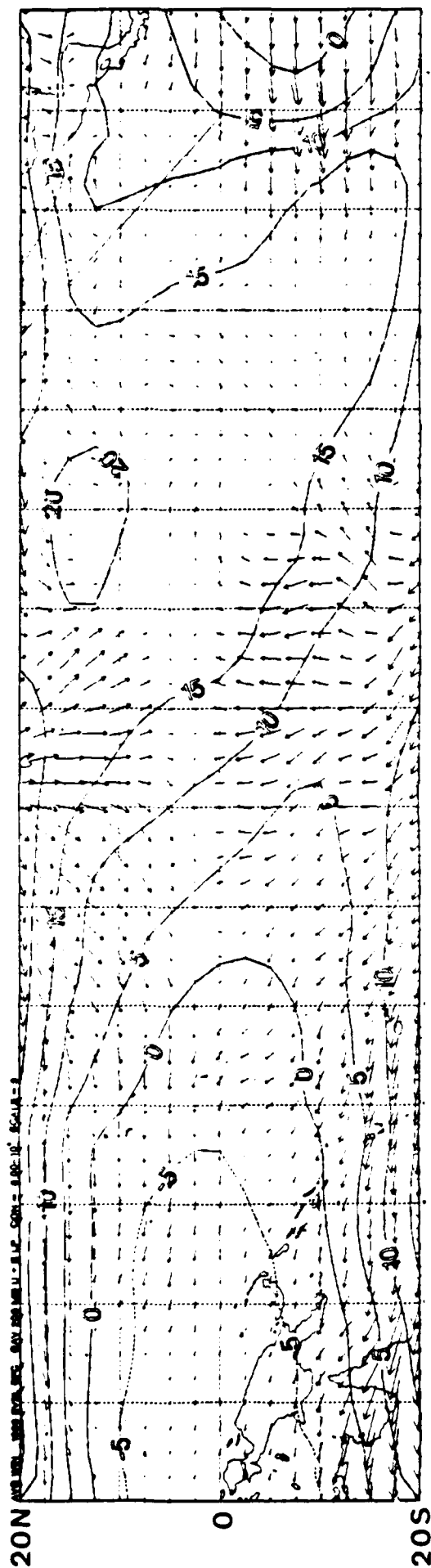
EV200 LPFILT DJF MEAN
1983 EV  CON= 5.87×10  TOT LAT=15.0 AVG=2
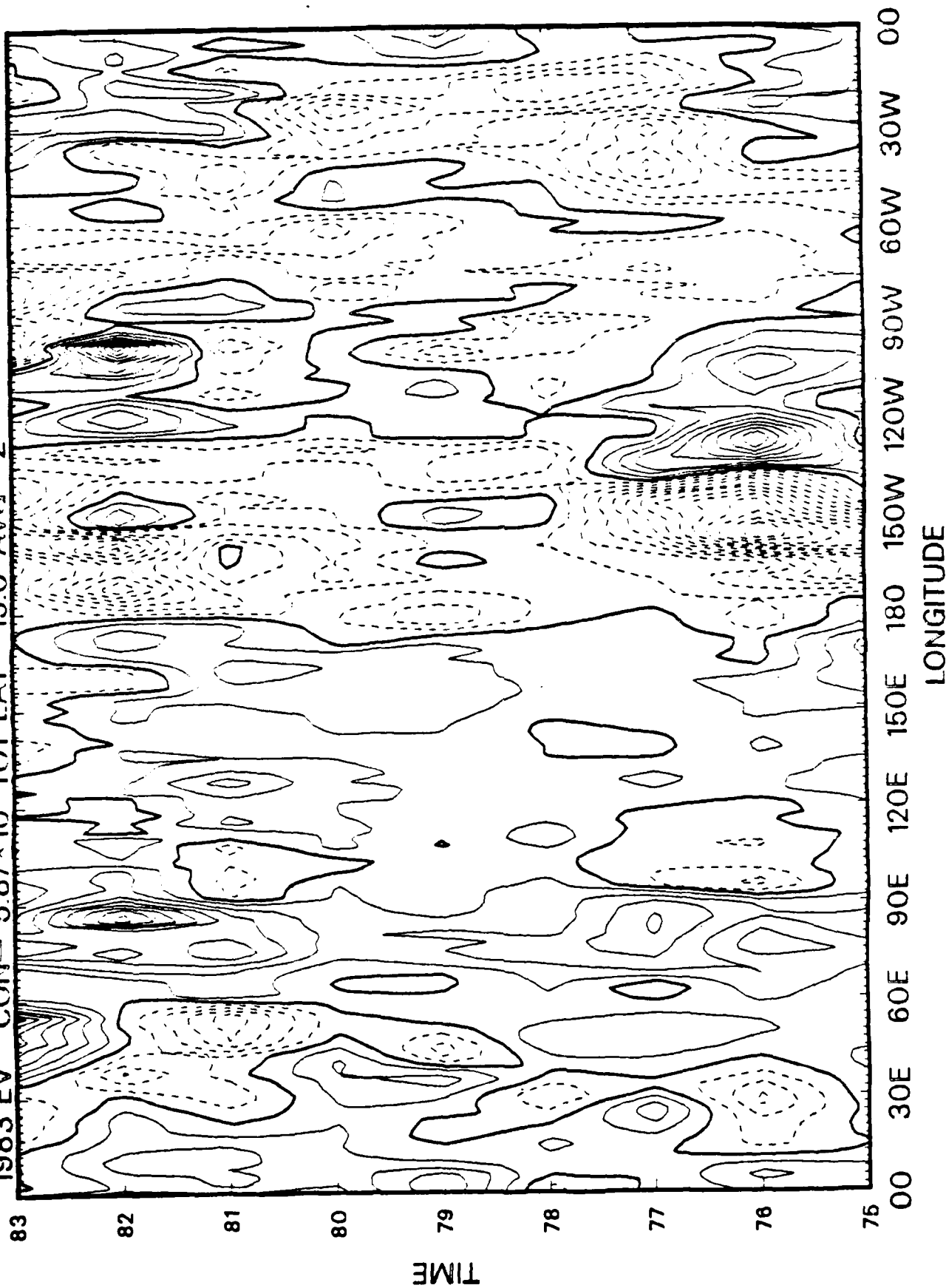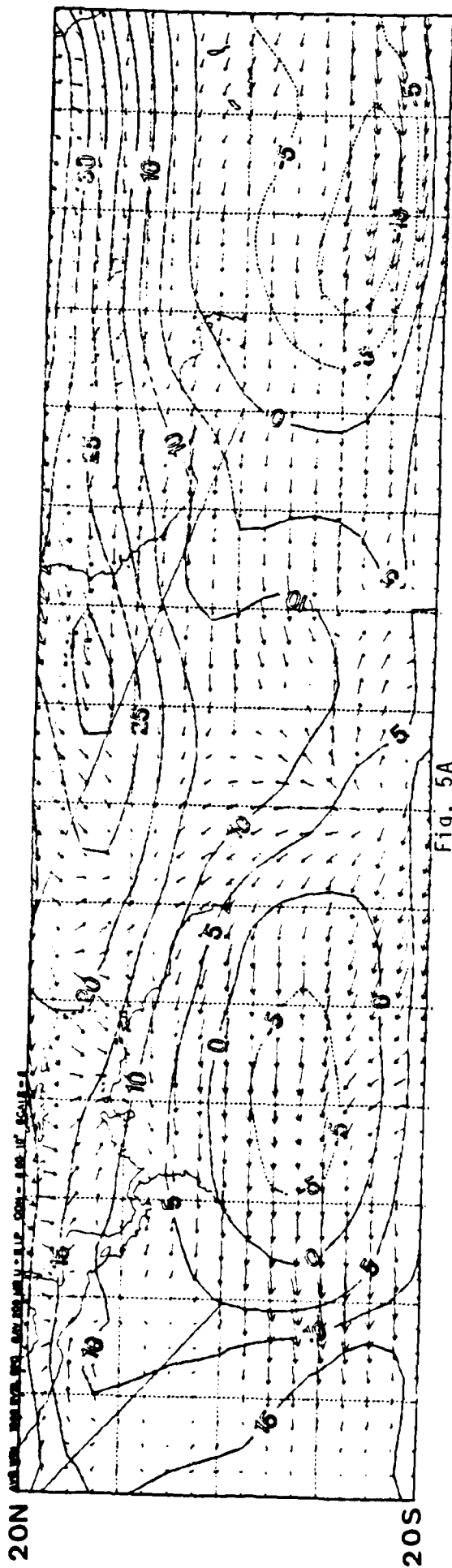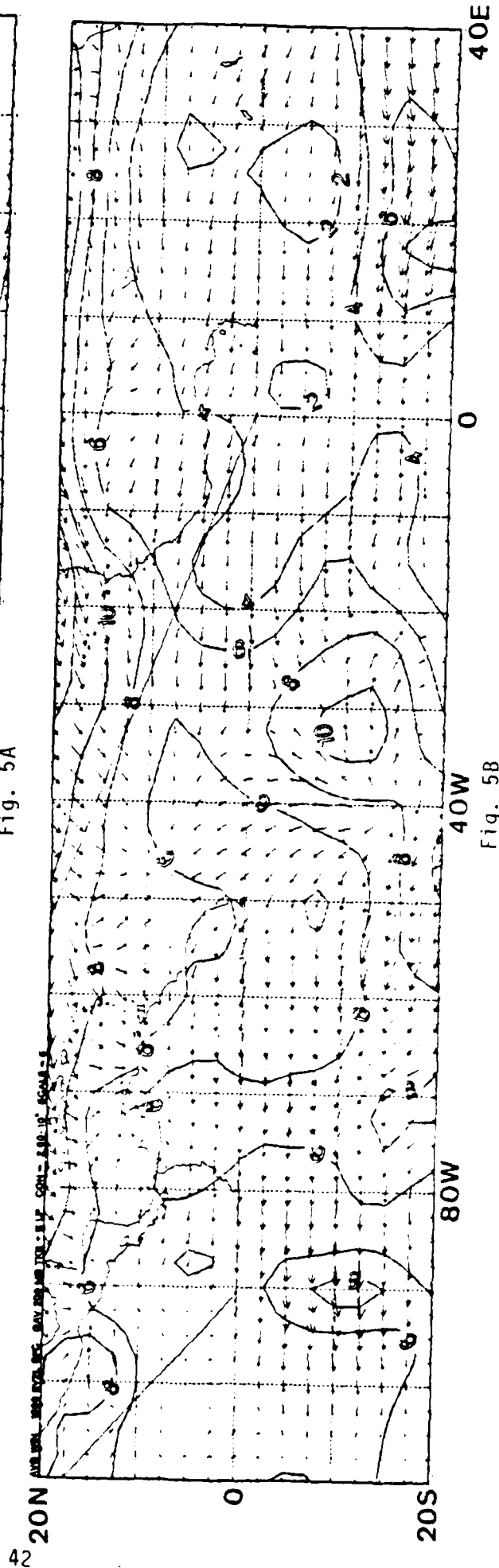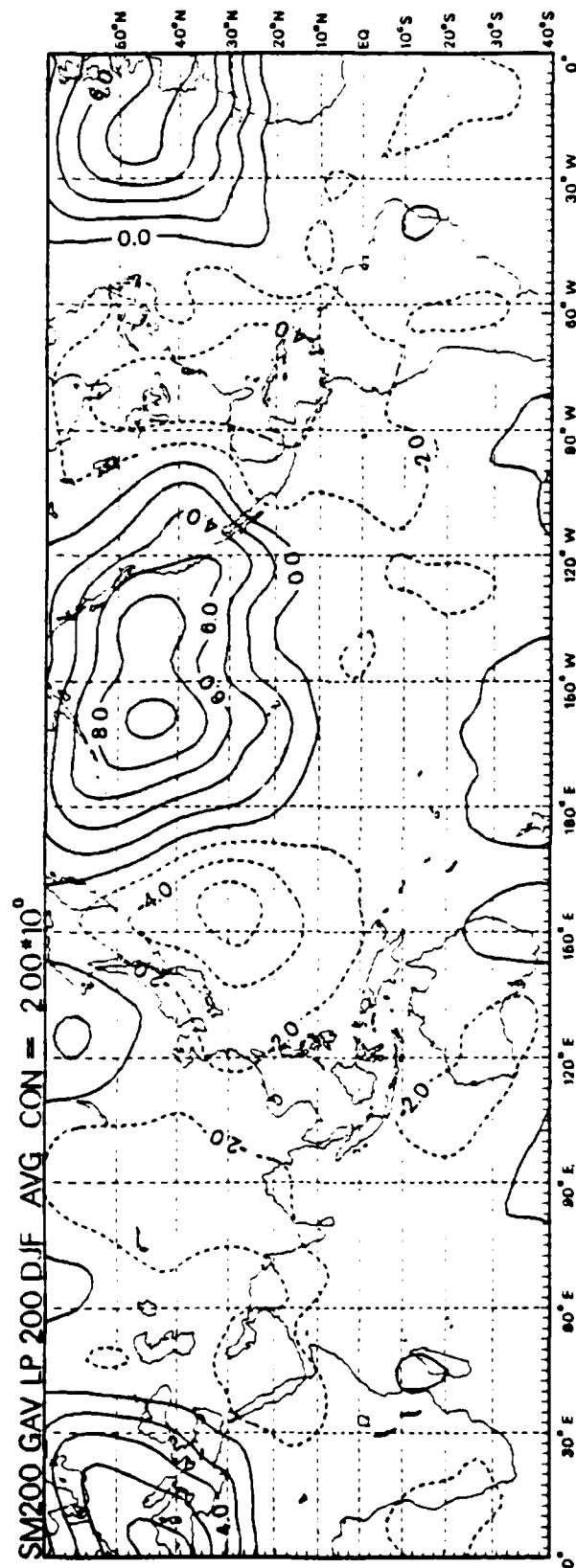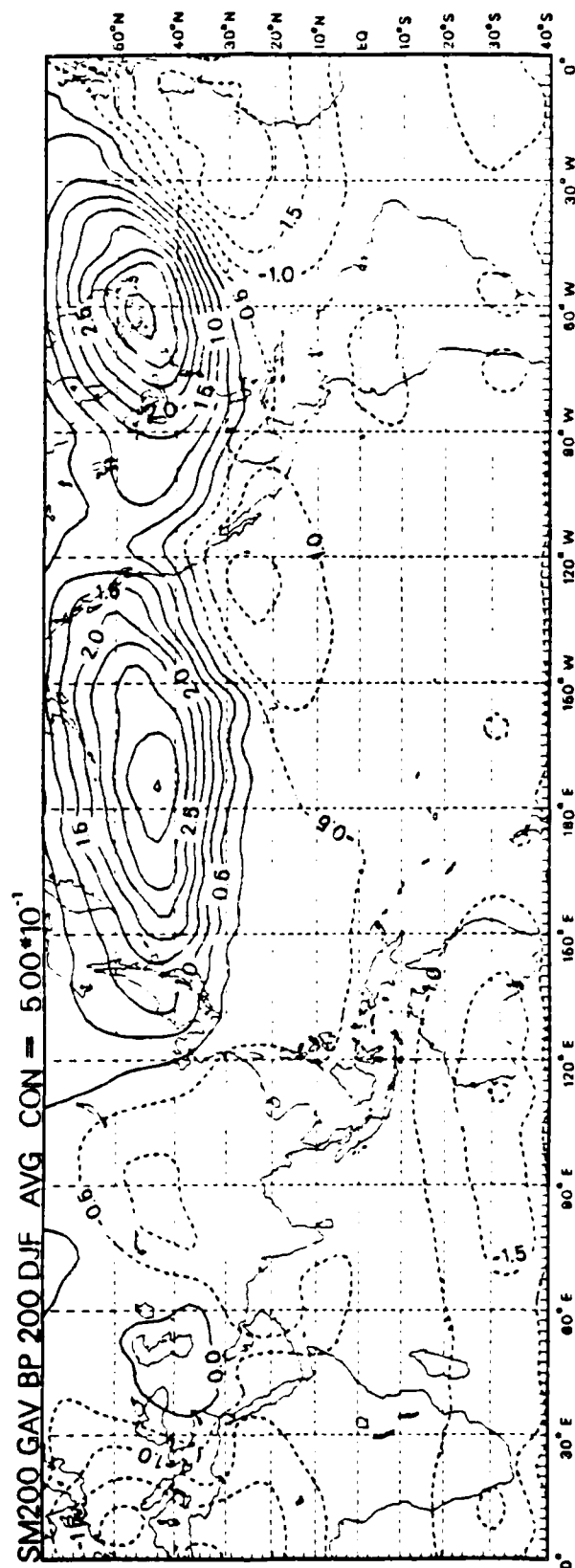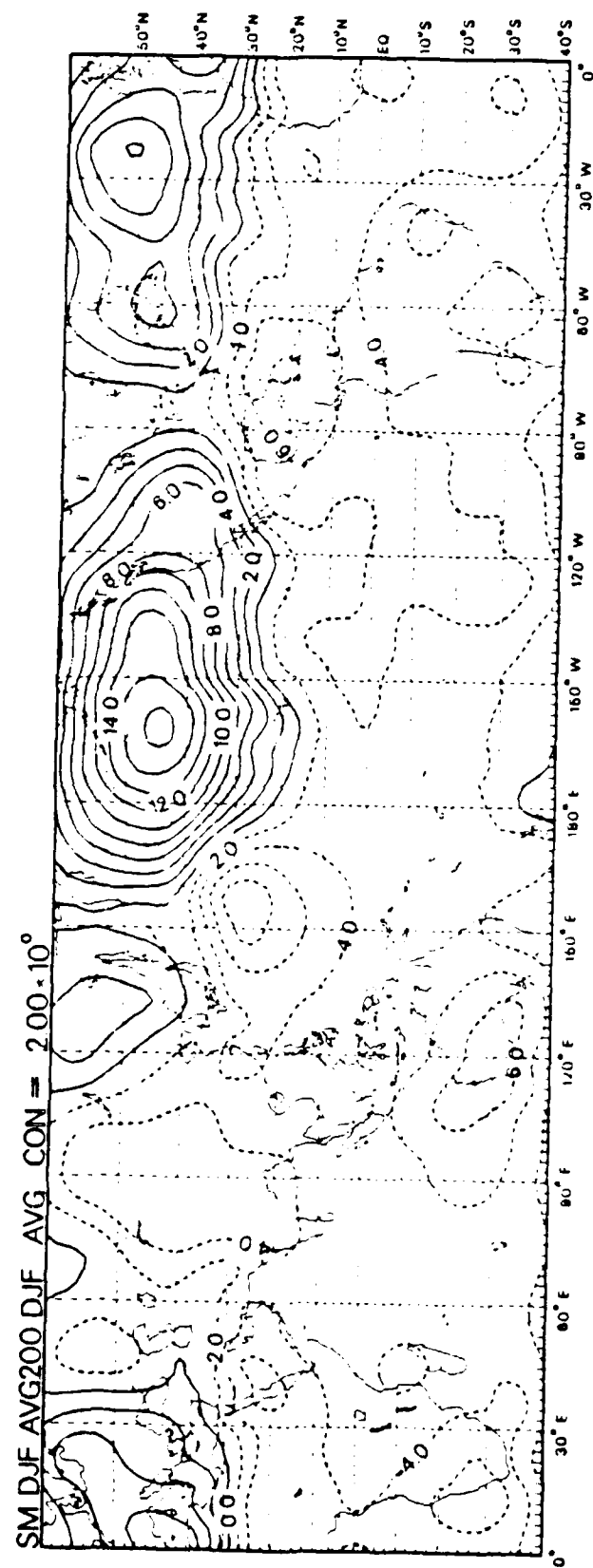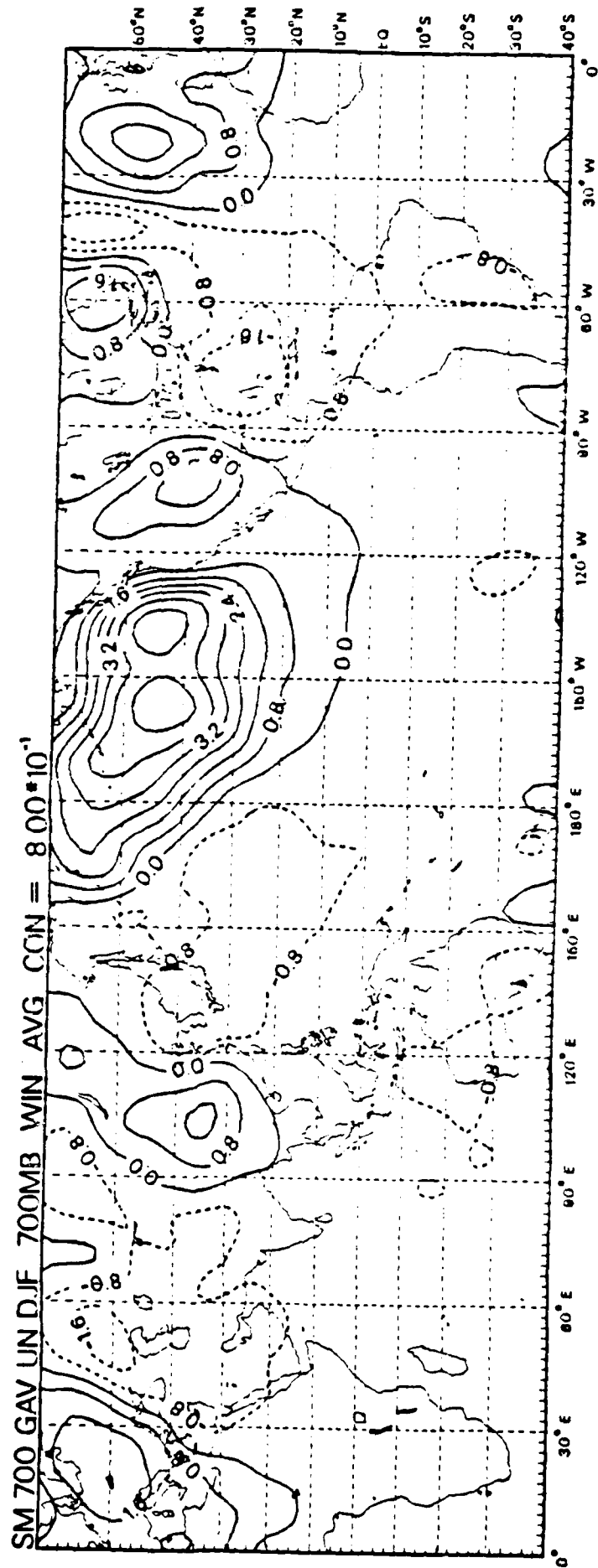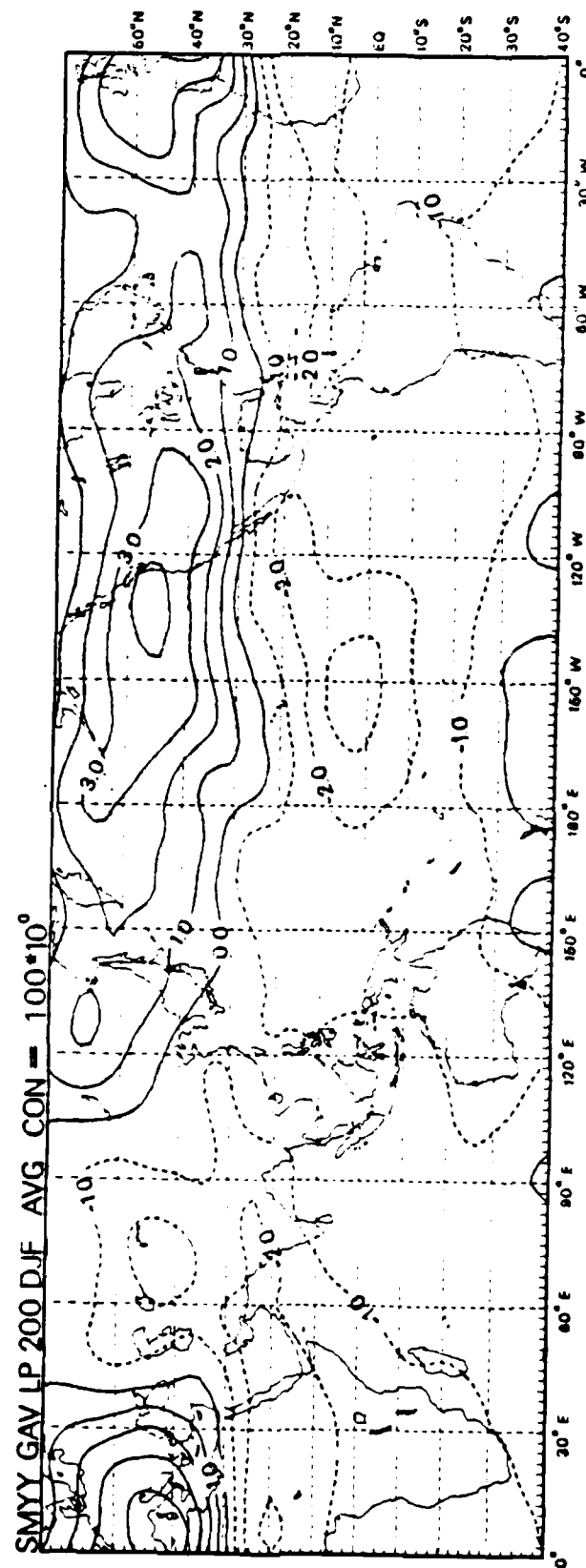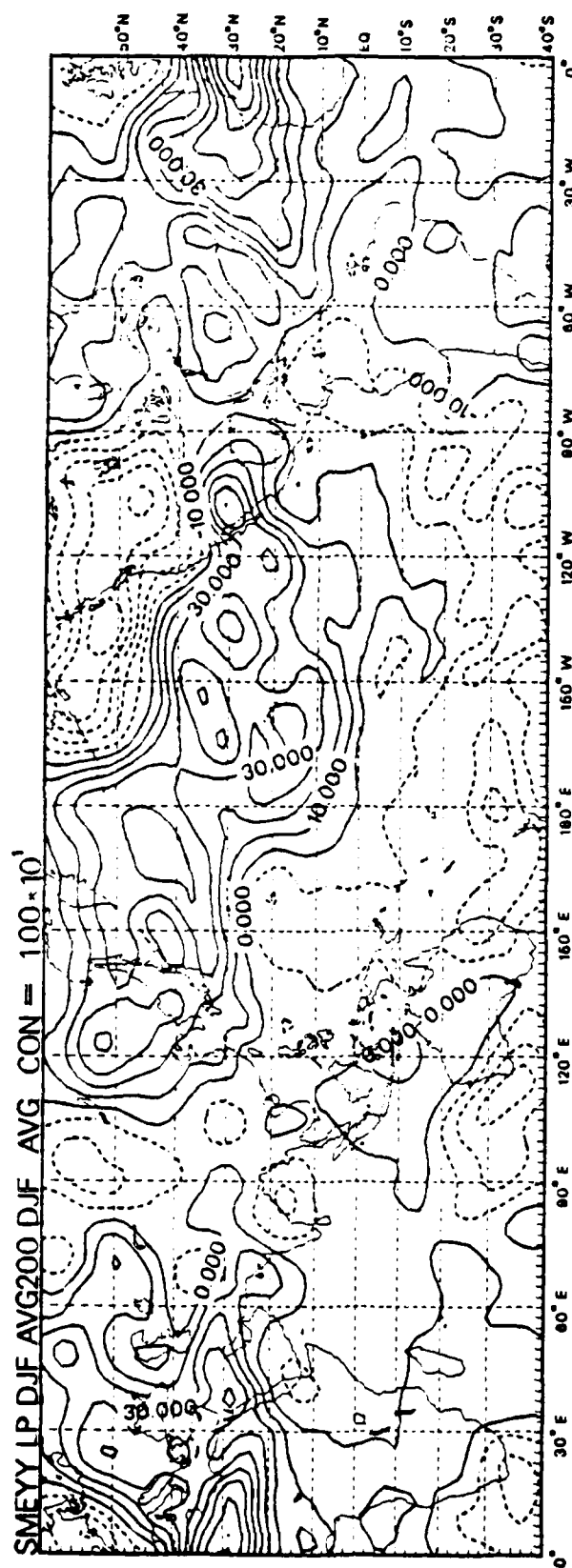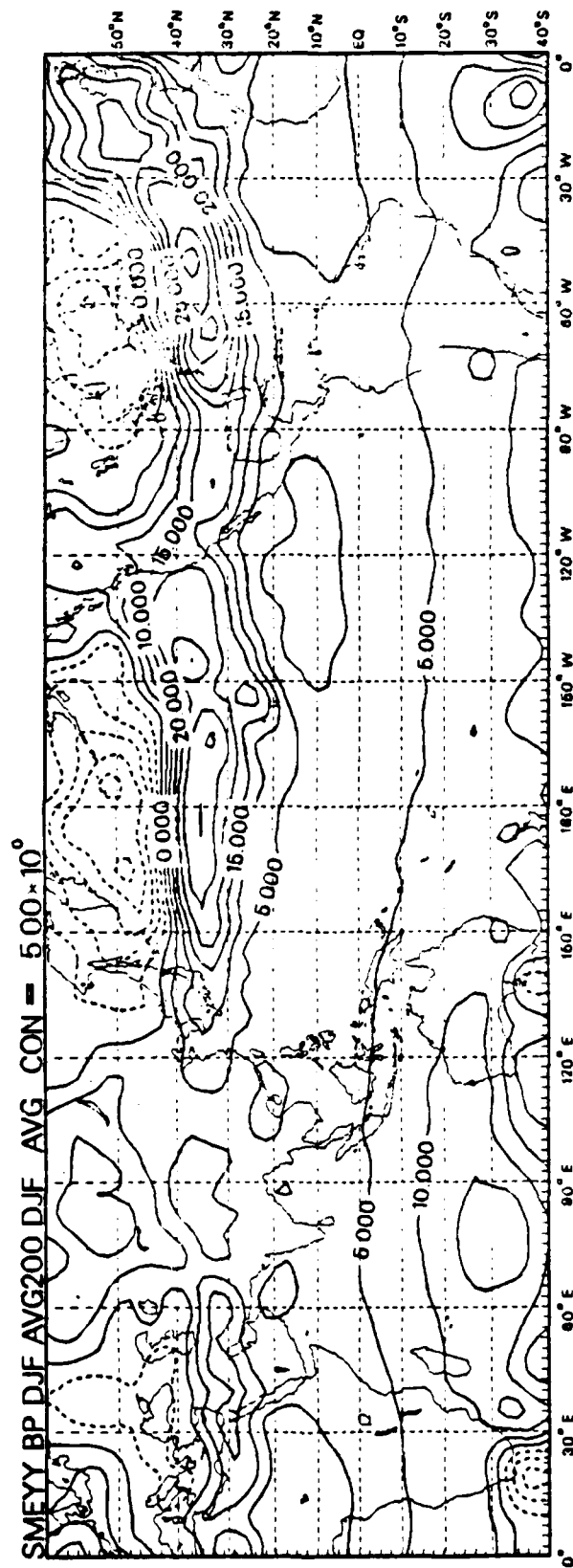
LONGITUDE

TIME

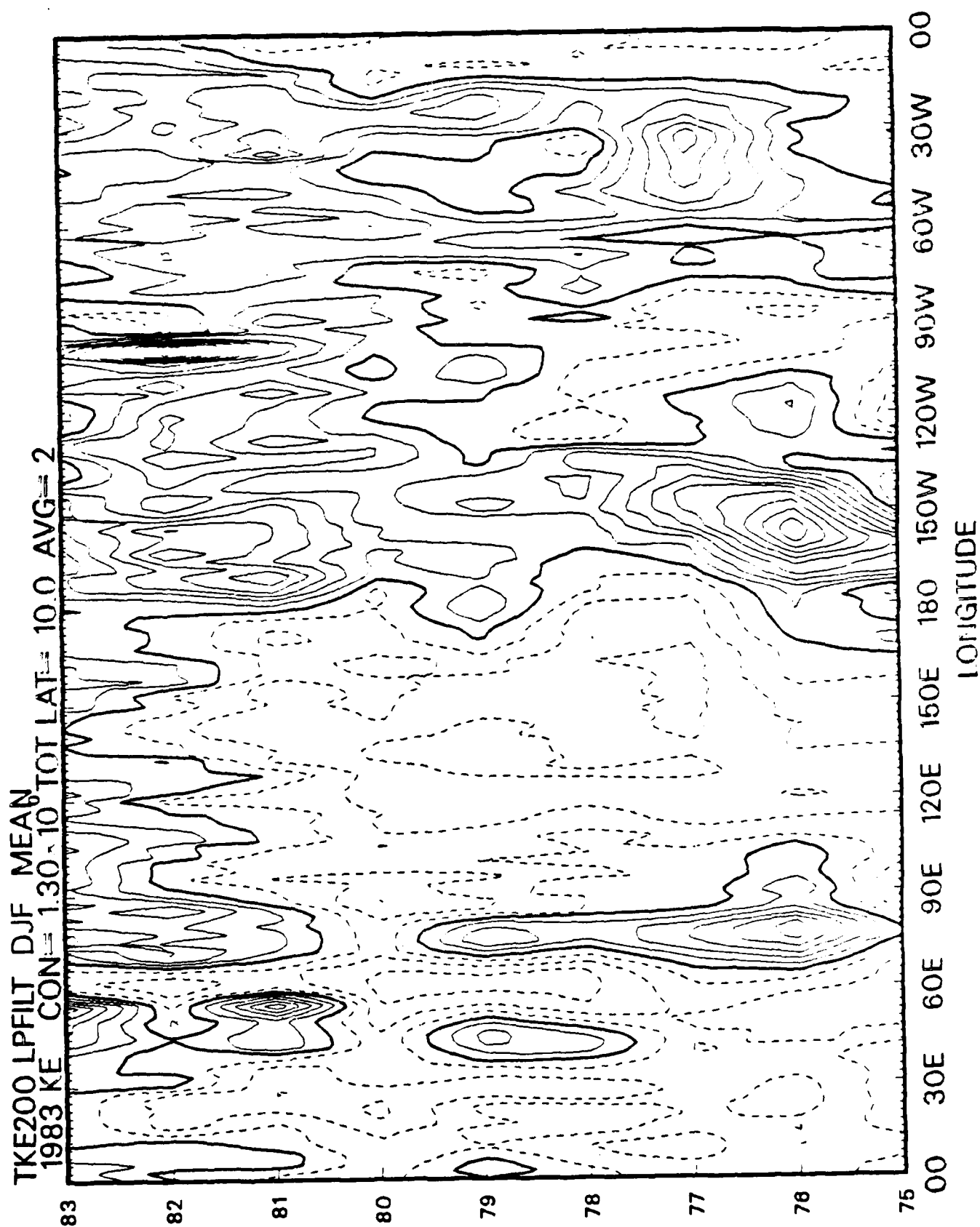TKE200 LPFILT DJF MEAN
1983 KE CON= 1.30×10 TOT LAT= 10.0 AVG= 2



Fig. 48

Fig. 5A

Fig. 5B

SM200 GAV LP 200 DJF  AVG  CON = 2.00*10⁰

Fig. 6A

43

SM200 GAV BP 200 DJF AVG CON = 5.00*10⁻¹

Fig. 6B

44

Fig. 6C

45

SM 700 GAV UN DJF 700MB WIN AVG CON = 8.00*10⁻¹

FIG. 7

46

SMYY GAV LP 200 DJF AVG CON = 100*10⁰

Fig. 8

47

SMEY LP DJF AVG200 DJF  AVG  CON =  100 * 10¹

Fig.  9A

Fig. 9B

SMEYY BP DJF AVG200 DJF AVG CON = 5.00×10⁰

49

SMEYY UN DJF AVG200 DJF AVG CON = 150×10¹

Fig. 9C

50

Fig. 10

51

SE200 GAV LP 200 DJF AVG CON = 2.00*10°

Fig. 11A

52

SE200 BP GAV200 DJF AVG CON = 2.00×10⁰

Fig. 11B

53

SE200 UN GAV200 DJF AVG CON = 2.00×10⁰

FIG. 11C

54

TKE GAV LP SEC DJF  AVG CON = 5.00*10⁻¹

Fig. 12A

TKE BP DJF AVGSFC DJF AVG CON = 5.00· 10⁻¹

Fig. 12B

56

TKESFC GAV UN SFC DJF  AVG  CON = 100*10⁰

Fig. 12C

57

7-S SHEAR UN AVG7-S DJF AVG CON = 2.00×10⁰

Fig. 13

# Part 2
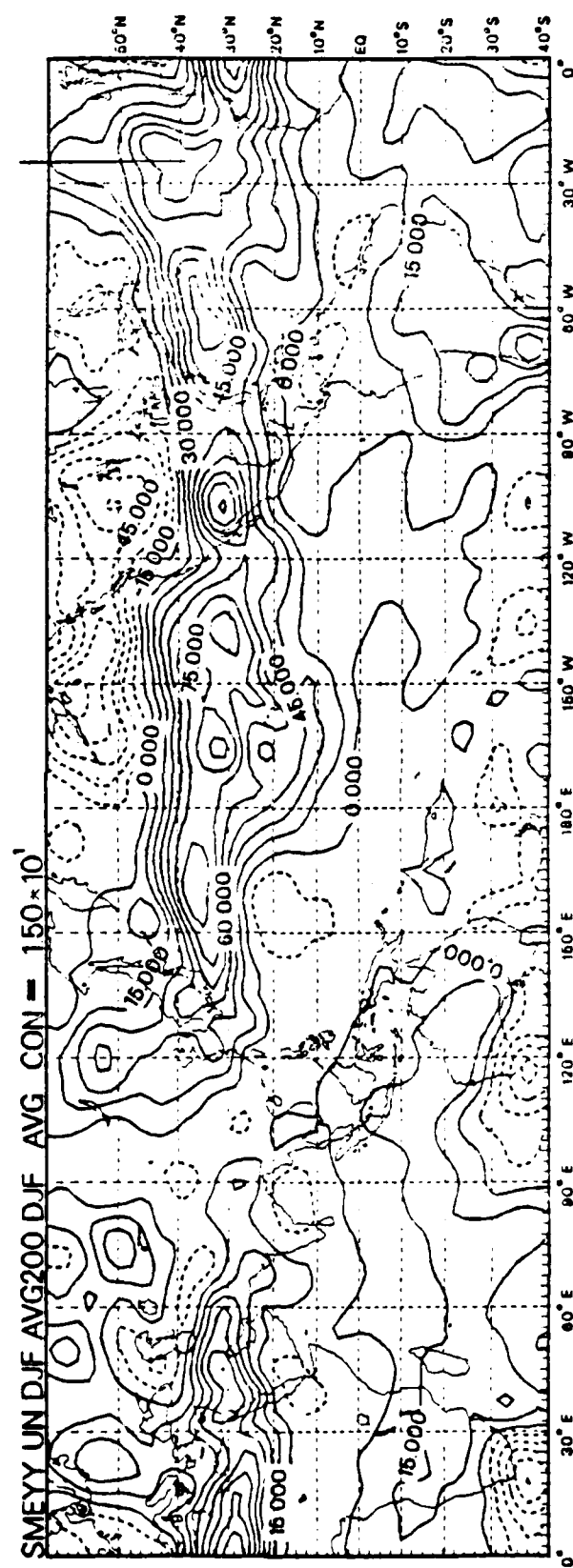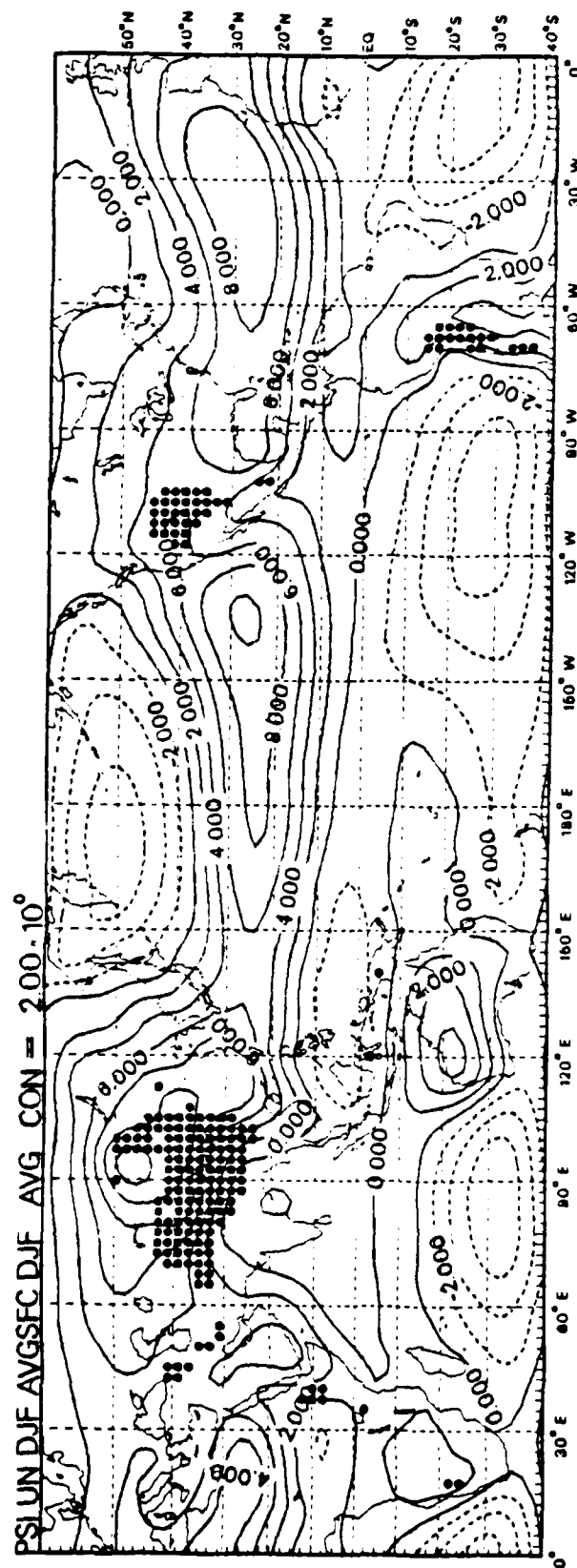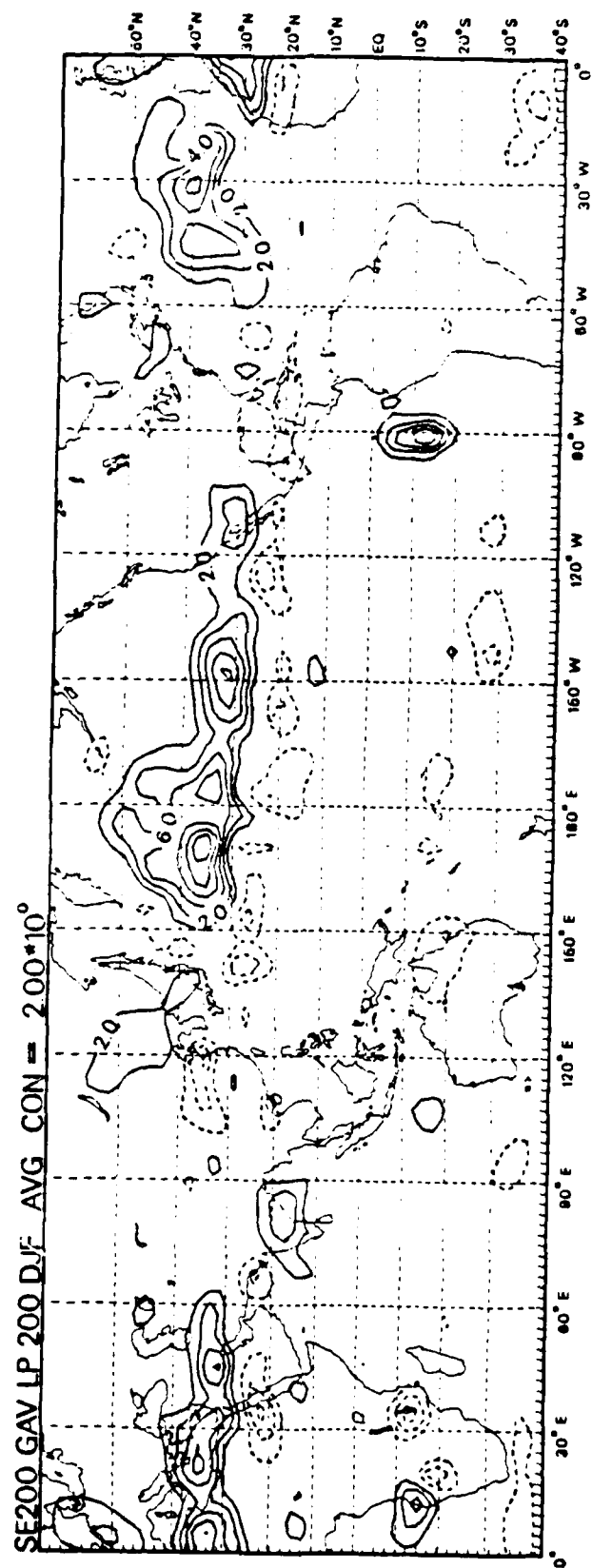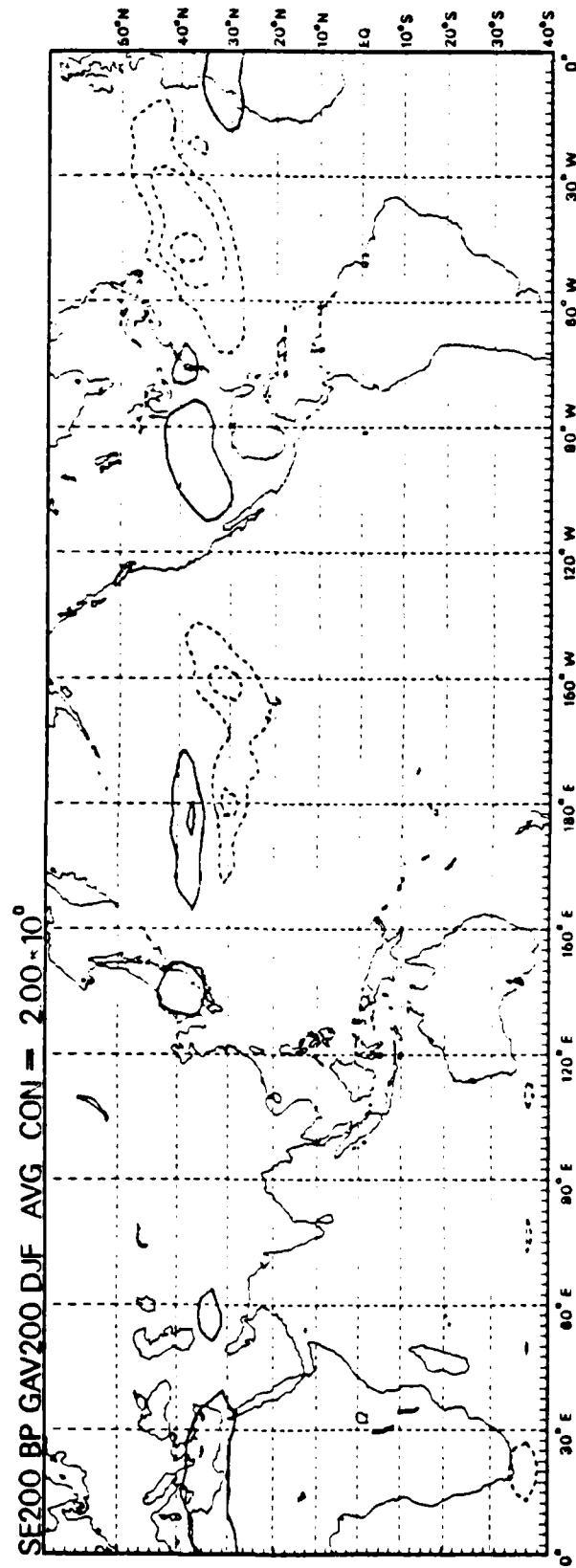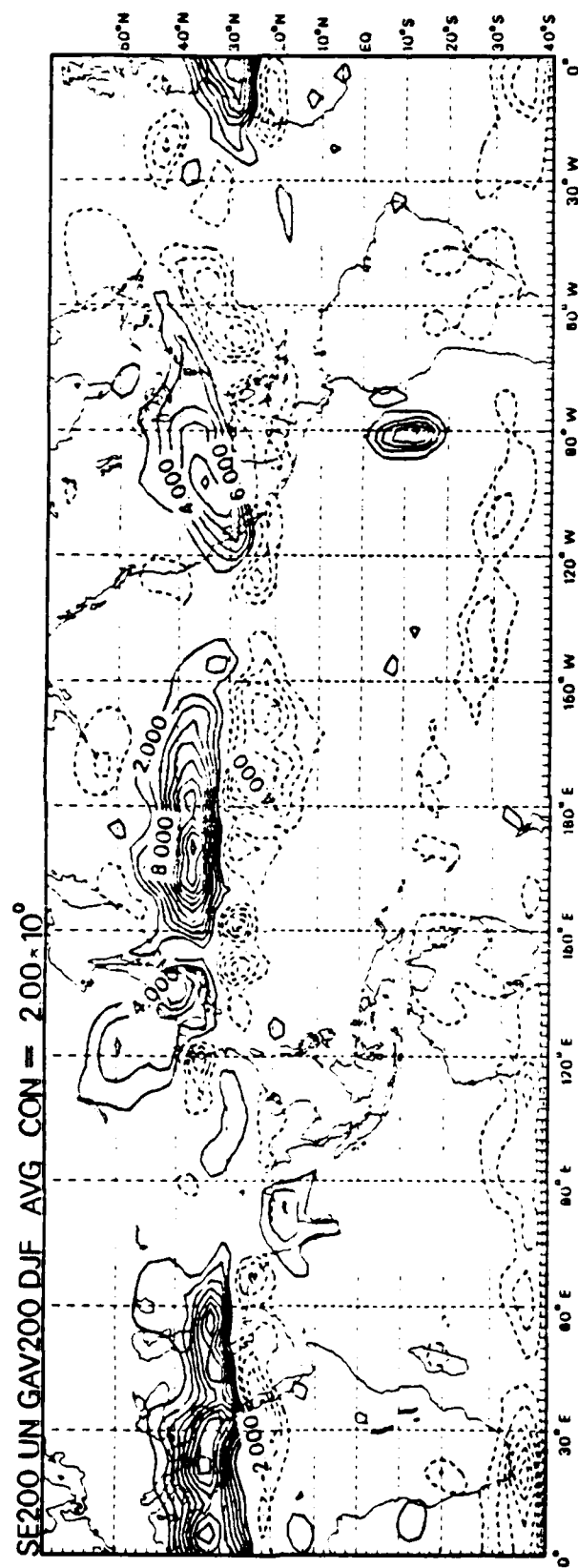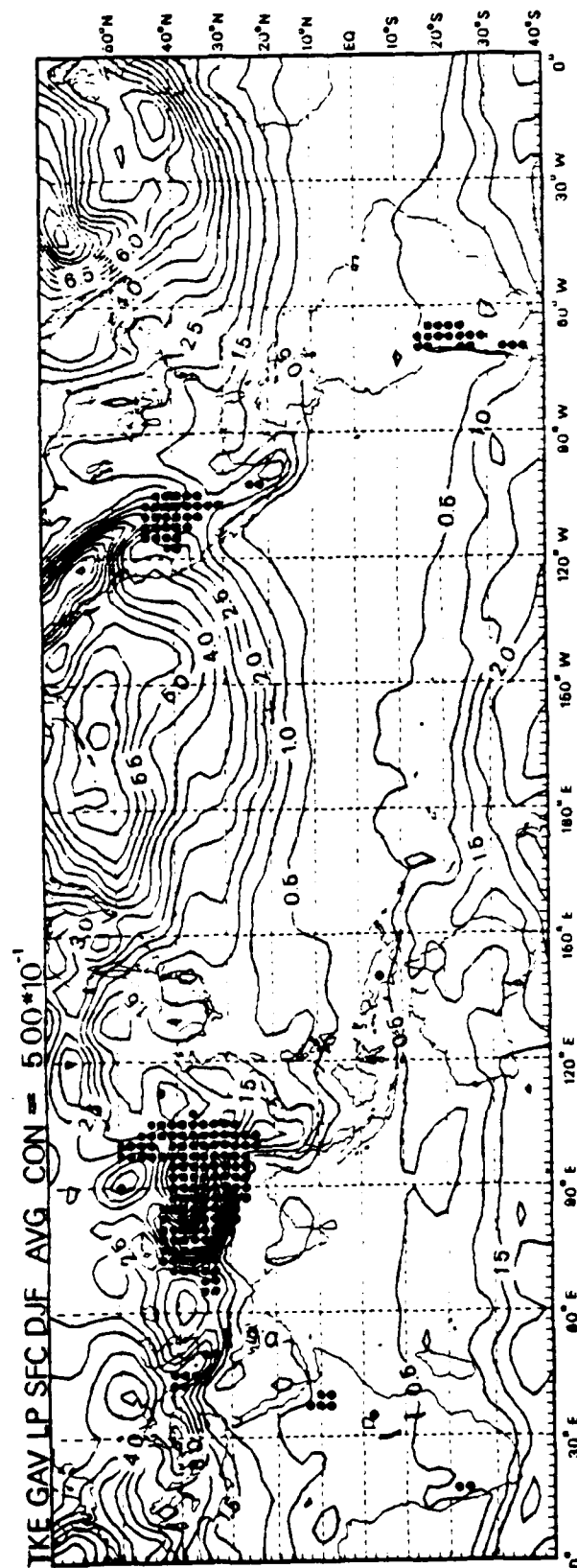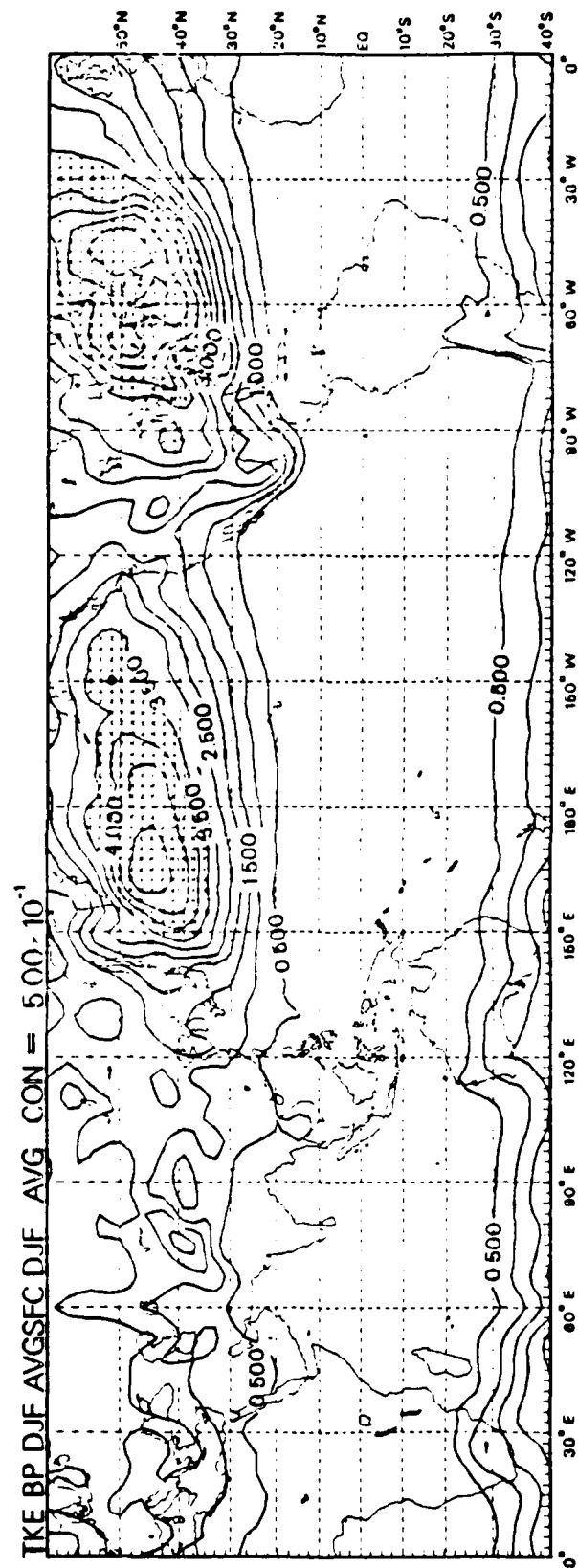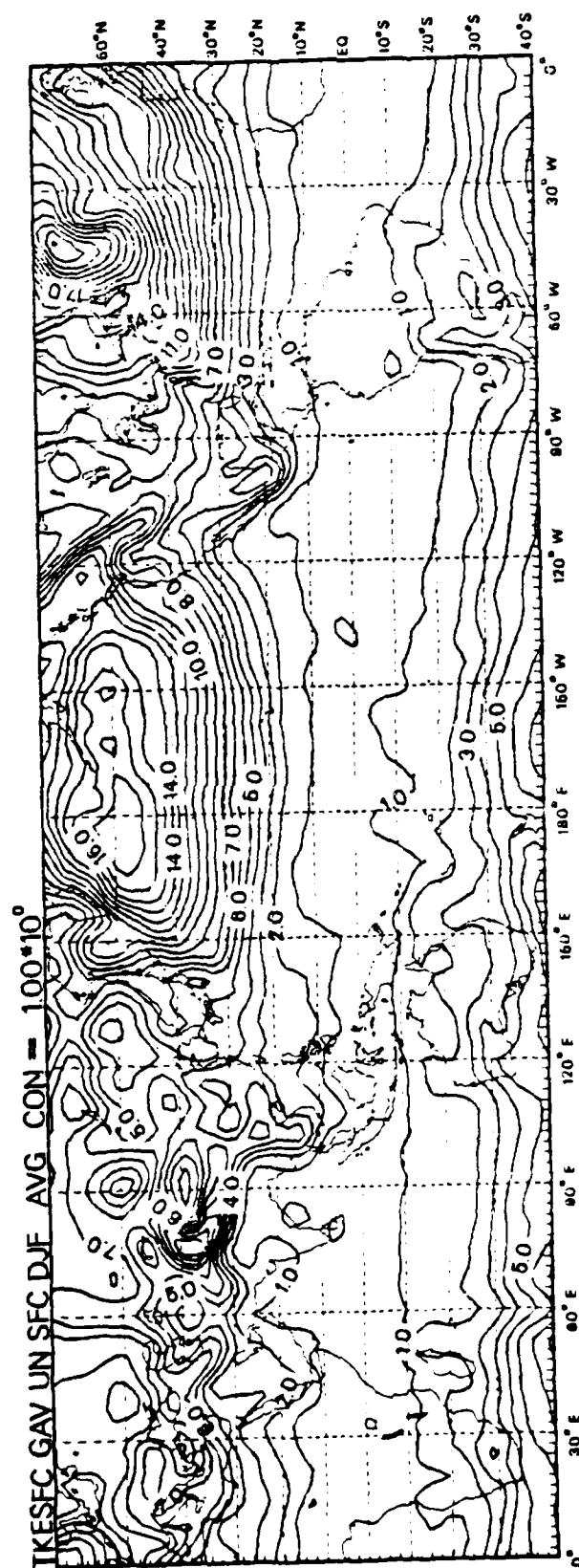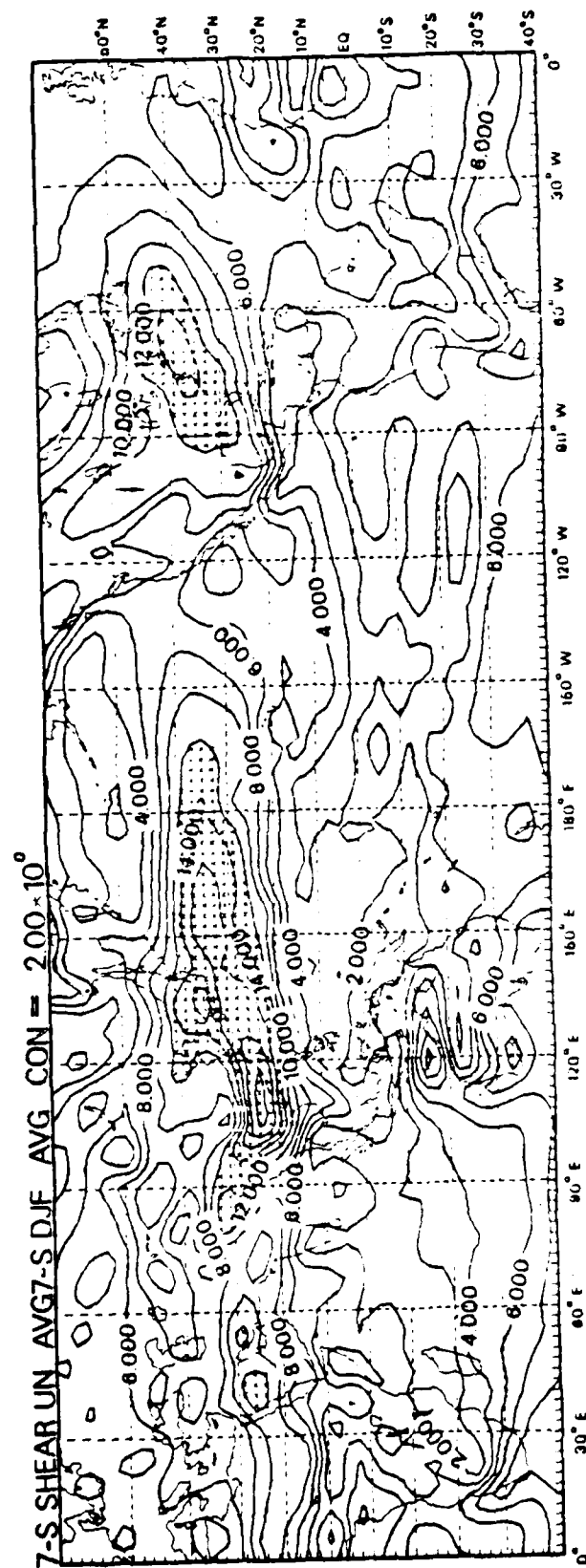
## Observational study of the divergent flow for the tropics and midlatitudes in the northern wintertime for the period 1974/75 to 1982/83

### ABSTRACT

A nine-year data set of U. S. Navy operational, twice-daily wind analyses at 200 mb, 700 mb and the surface from $60^{\circ}N$ to $40^{\circ}S$ is used to compute divergent wind during the northern winter(December, January, February).

The divergent wind fields at the surface, 700 mb and 200 mb are in good agreement in the Tropics and sub-Tropics with the observed OLR fields. The agreement is good in the sense that upper-level divergence and lower level convergence is associated with low values of OLR, the assumption being that low OLR values are areas of vertically developed cumulus. Comparison of the surface and 700 mb patterns of velocity potential, indicates that the deepest region of low-level convergence is found over the maritime continent of Indonesia.

Estimates of the ageostrophic wind using the time averaged vorticity equation at 200 mb are in agreement in mid-latitudes with the work of Lau (1979) and Blackmon et. al. (1977). Comparison of the ageostrophic estimates and the divergent wind indicates the former is not a very good estimate of the latter. As Blackburn (1985) points out, studies which infer vertical motion from the ageostrophic fields may not be on solid ground.

# I. INTRODUCTION

Presented here are time mean fields of the divergent wind and velocity potential at 200 mb, 700 mb and the surface. These fields can be compared to the results of Arkin et. al. (1986) and Krishnamurti et. al. (1973). One aspect here is to compare the analysed divergent circulations to the estimates of ageostrophic wind derived from the time mean zonal momentum budget. The work of Blackburn (1985) indicates that these two fields should be quite different, and he emphasises the dangers of inferring the divergent flow from the ageostrophic estimates. Also, it is of interest to investigate how the centers of action in the divergent wind field fit into the pattern jet maxima.

In this paper the data source and computation procedures are described in Section 2. Section 3 presents the nine-year means of the velocity potential and the divergent wind. The results are compared to previous calculations and interpreted in light of what is known of tropical convection. Section 4 presents the relations of the divergent centers to the jet maxima and and compares this to estimates of the ageostrophic wind. Section 5 contains concluding remarks and a summary of the results.

# II. DATA AND CALCULATIONS.

The wind data used in this work are the operational analyses of the Numerical Variational Analysis (NVA) produced by the U. S. Navy's Fleet Numerical Oceanography Center (FNOC). The details of the FNOC analysis procedures are described in Part I. Of importance is the fact that the FNOC procedures

are such that no attempt was made to alter the divergence that was analysed in the wind fields. Thus the FNOC data represents the longest running operational system containing information about the divergent wind. A significant portion of the day to day changes in this divergent wind was found to be consistent with physically meaningful processes in work by Chang and Lau (1980, 1982), Lau et. al. (1983) and Chang and Lum (1985).

## A. Computation of velocity potential

The velocity potential ( $\chi$ ) was computed following the procedures described by Chang and Lau (1980, 1982).

In addition, the windfield was directly decomposed into its rotational and divergent components using the method of Endlich (1967). This method does not require any assumption about the boundary conditions. The divergent wind vectors shown in the following figures are not computed from the velocity potential but are those computed by the Endlich technique. The excellent agreement between the $\chi$ field and the divergent winds over the entire grid, gives additional confidence in the accuracy of the computations.

## III. TROPICAL DIVERGENT FLOW AND CONVECTION.

Figure 1 presents the nine-winter mean velocity potential and divergent wind at 200 mb, 700 mb and the surface. In the tropics the divergence fields are often compared with the outgoing long wave radiation

(OLR) under the assumption that low values of OLR imply the presence of deep, persistent convective clouds (Gruber and Krueger, 1984). The nine-winter mean OLR is plotted in Figure 2

The 200 mb divergence has been calculated by several investigators, including Krishnamurti et. al. (1973) and Murakami and Unninayar (1977), both for a single winter only, and Arkin et. al. (1986) for a five-winter period from 1978/79 to 1982/83. The latter two studies used the NMC operational analysis. All these works show a strong east-west (Walker-type) divergent component which is at least comparable to the north-south (Hadley-type) component. However, our result shown in Figure 1 indicates a more prominent Hadley-type component at 200 mb. This is manifested by a better defined South Pacific Convergence Zone (SPCZ) as compared with previous studies; the SPCZ outflow corresponds reasonably well to the minimum OLR pattern in Figure 2. There are also in general more smaller scale details especially compared to the NMC data based calculations. This difference is perhaps due to the influence of the NWP model forecasted divergence in the NMC analysis. An example is the outflow zone in the equatorial eastern Pacific centered near 121W. This area is totally absent in Murakami and Unninayar (1976) and Arkin et. al. (1986), but is present in Krishnamurti et. al. (1973) who based their calculations on a subjective analysis of the January -March 1969 data. This divergence feature may be compared to a narrow band of minimum OLR immediately west of 120W, which is the only stippled ( < 225 Wm$^2$) area in the entire tropical eastern Pacific in Figure 2. Other significant differences from the NMC based studies include the locations of the divergence center over South America and Africa. They are centered near the

equator in the NMC based analyses, while in Figure 1a they are near 10S, in good agreement with the OLR minima in Figure 2 The one feature that shows up in Figure 1 but cannot be identified with an obvious corresponding feature in the OLR chart is the smaller scale, secondary divergence center in the Arabian Sea/Indian Ocean.

The more detailed structure in the 200 mb divergence is, in general, consistent with the 700 mb ( Figure 1b) and the surface ( Figure 1c) convergence areas where large-scale deep convection is indicated in the OLR. This includes the SPCZ, and the equatorial South American and African convergence zones. Among the above mentioned divergence calculations, only Murakami and Unninayar (1976) showed the 700 mb fields. The main difference shown in our 700 mb results are similar to those found at 200 mb, including the more prominent Hadley-type flow, a much better defined SPCZ and greater detail. The correspondence of our data with the OLR, especially the 200 mb divergence and the surface convergence, is at least an indirect confirmation of the veracity of the divergent wind described in this data.

There are significant geographical differences in the vertical structure of the low-level divergence. Generally, there is a decrease of the divergent wind magnitude in going from the surface ( Figure 1c) to 700 mb ( Figure 1b). The largest values of $\chi$ are found in the equatorial western Pacific. It may be worth noting that, in a study of rawindsonde data in summer 1973, Thompson et. al. (1979) found that the divergence diminished rapidly with height in the GATE B-scale ship hexagon but does not change much in the Kwajalein-Enewetok-Ponape triangle in the western Pacific. It would appear that the two

major convective centers over equatorial Africa and South America have their low-level convergence largely restricted to below 700 mb.

An interesting feature of the SPCZ as depicted in Figure 1 is that there is a slightly closer relation between the 200 mb divergence and the 700 mb convergence than the surface convergence. Both the 200 mb and the 700 mb fields clearly show the west-northwest to east-southeast orientation which is not obvious in the surface convergence zone. This orientation has been well known from satellite pictures and shows up in the OLR. Thus, it appears that certain intrinsic features of the SPCZ are not forced by surface based processes.

## IV. SUBTROPICAL JETS.

### A. Divergence patterns about the jet maxima.

Figure 3 is a plot of the 200 mb divergent wind vectors and contours of the 200 mb zonal wind. With respect to the upper-level wind features, the EAJ and NAmJ have convergence on the cyclonic side of the entrance region and divergence on the cyclonic side of the exit region. The 200 mb and surface patterns tend to be of opposite sign indicating deep vertical motions. The vertical motions inferred from the 200 mb and surface fields are broadly comparable to the patterns of omega displayed by Lau et. al. (1981), This vertical motion field was derived from the operational NMC models which only provided data north of $20^{\circ}$N. The NAfJ does not show any of the signs of the divergence patterns associated with the EAJ and NAmJ.

The divergence maxima in the NAmJ exit is over the TKE surface band pass maxima, Boyle and Chang (1987), which is not the case for the EAJ. The TKE surface band pass maximum associated with the NAmJ is of greater magnitude than that of the EAJ. The surface convergence zones across the northern Pacific and Atlantic are coincident with the surface transient kinetic energy maxima (Fig. 3, Boyle and Chang, 1987). This indicates that the convergence associated with the strong cyclones in this region dominates in the long term mean.

In the northern midlatitudes the data of Figure 1a is in good agreement with the NMC data of Arkin et. al. (1986). In both sets of data there are convergence (divergence) centers in the left entrance (exit) regions of the EAJ and NAmJ. In Figure 1a both centers associated with the EAJ lie along 35N, while the centers of the NAmJ tilt southwest to northeast from 35N to about 52N. This is in keeping with the orientation of the jet axis. The velocity potential and divergent winds of Lau(1979, Fig. 13) is similar to Figure 1a for the NAmJ but his data show strong northerly divergent wind in the EAJ exit, while our data ( and Arkin et. al., 1986) have easterly to southeasterly divergent winds. Lau (1979) has a major convergence center at 170E, 25N but is missing the divergence center east of the dateline at 35N seen in Arkin et. al. (1986) and in Figure 1a. Lau's (1979) values were deduced using a vorticity budget technique on the NMC wind analysis. Lau could only compute values poleward of 25N due to data limitations. As mentioned in the section above the fields of Arkin et. al. (1986) and Figure 1a. are quite different in the Tropics, yet they are quite similar in midlatitudes especially in the disposition of the convergence divergence centers about the major jet maxima.

## B.    Divergent versus ageostrophic flow.

The acceleration of the zonal wind may be expressed as

$$D(u)/Dt = fv_a$$

or

$$\partial u/\partial t + u\partial u/\partial x + v\partial u/\partial y \sim f(v - v_g). \qquad (1)$$

For a long term average, $\partial u/\partial t$ is approximately zero. The actual balance as shown by Lau (1979) and Blackmon et. al. (1977) is mainly between the zonal advection and the coriolis torque.

Given that the flow about the jets is for the most part horizontal and zonal at 200 mb and that the divergent wind is a good approximation to the ageostrophic wind, one would expect poleward divergent flow in the entrance regions to the jet maxima (where $u\partial u/\partial x < 0$) and equatorial divergent flow in the exit regions. That this is generally the case is apparent from Figure 1a, and Figure 2. The EAJ does appear to have southerly divergent flow in the entrance region but no clearly organized northerly values in

66

the exit region. The NAfJ has evidence of positive values in the entrance and negative in the exit. The NAmJ has definitely positive entrance values if the entrance is considered as extending to the southwest of the Baja Peninsula.

Of course, expecting such a simple picture about the time mean jet is rather naive. Blackburn(1985) has shown a significant amount of the ageostrophic flow is contained in the rotational component of the wind. He has shown that for the winter of 1982/83 the cross contour flow which forms a couplet about the EAJ is for the most part is due to the rotational wind. That the rotational wind is important in the local generation of kinetic energy was shown by Krishnamurti (1968).

The time mean ageostrophic flow can be estimated using the zonal momentum equation as follows:

$$f(\bar{v} - \bar{v}_g) \sim \bar{u}\partial\bar{u}/\partial x + \bar{v}\partial\bar{u}/\partial y + \partial(\overline{u'u'})/\partial x + \partial(\overline{u'v'})/\partial y \qquad (2)$$

where the overbars indicate a long term time average and $\partial\bar{u}/\partial t$ is assumed to be negligable. The right hand side of (x) was computed and the results are displayed in Figure 4. The pattern is very similar to that of Lau (1979) who performed a similar computation on a different data set. The fields about the jet maxima are dominated by the $u\partial u/\partial x$ term, as found by Lau. For comparison Figure 5 presents the product of the coriolis parameter and the meridional divergent wind ($fv_\chi$). The $v_\chi$ was computed by the

67

method of Endlich described in Section 3. There is some similarity between the $fv_a$ and $fv_\chi$ fields in the subtropics but the correspondence degenerates quickly poleward. Even in the subtropics the agreement across Northern Africa is non-existent. This poor correspondence between the fields could be anticipated from the results of Blackburn (1985). This highlights the dangers of inferring the divergent (vertical motion) circulations from estimates of the ageostrophic wind.

## V. SUMMARY AND CONCLUSIONS.

1.  The divergent wind fields at the surface, 700 mb and 200 mb are in good agreement in the Tropics and sub-Tropics with the observed OLR fields. The agreement is good in the sense that upper-level divergence and lower-level convergence is associated with low values of OLR, the assumption being that low OLR values are areas of vertically developed cumulus. Comparison of the surface and 700 mb patterns of velocity potential, indicates that the deepest region of low-level convergence is found over the maritime continent of Indonesia.

2.  Estimates of the ageostrophic wind using the time averaged vorticity equation at 200 mb are in agreement in mid-latitudes with the work of Lau (1979) and Blackmon et. al. (1977). Comparison of the ageostrophic estimates and the divergent wind indicates the former is not a very good estimate of the latter. As Blackburn (1985) points out, studies which infer vertical motion from the ageostrophic fields may not be on solid ground.

68

# REFERENCES

Arkin, P. A., V. E. Konsky, J. E. Janowiak, and E. A. O'Lenic, 1986: *Atlas of the tropical and sub-tropical circulation derived from National Meteorological Center Operational Analyses,* NOAA Atlas No. 7, Silver Spring , MD 8pp. (Copies can be obtained from: Climate Analysis Center, 5200 Auth Road, Washington D. C. 20233)

Blackburn, M. 1985: Interpretation of ageostrophic winds and implications for jet stream mainte-nance. *J. Atmos. Sci.,* **42,** 2604-2620.

Blackmon, M. L., J. M. Wallace, N.-C. Lau and S. L. Mullen, 1977: An observational study of the Northern Hemisphere wintertime circulation. *J. Atmos. Sci.,* **34,** 1040-1053.

Boyle, J. S. and C.-P. Chang, 1987: Observational study of the time mean flow and transients for the northern wintertime for the period 1974/75 to 1982/83. Submitted to *J. Atmos. Sci.*

Chang, C.-P., and K. M. Lau, 1980: Northeasterly cold surges and near-equatorial disturbances over the winter MONEX area during December 1974. Part II: Planetary scale aspects. *Mon. Wea. Rev.,* **108,** 298-312.

Chang, C.-P., and K. M. Lau, 1982: Short-term planetary-scale interactions over the tropics and midlatitudes during Northern winter. Part I: Contrasts between active and inactive periods. *Mon. Wea. Rev.,* **110,** 933-946.

Chang, C.-P., and K. G. Lum, 1985: Tropical-midlatitude interactions over Asia and the Western Pacific Ocean during the 1983/84 northern winter. *Mon. Wea. Rev.*,113, 1345-1358.

Cressman, G. P., 1959: An operational objective analysis system. *Mon. Wea. Rev.*, 87, 367-374.

Endlich, R. M., 1967: An iterative method for altering the kinematic properties of wind fields. *J. Appl. Meteor.*, 6, 837-844.

Gruber, A. and A. F. Krueger, 1984: The status of the NOAA outgoing longwave radiation data set. *Bull. Amer. Meteor. Soc.*, 65, 958-962.

Krishnamurti, T. N., 1968: A diagnostic balance model for studies of weather systems of low and high latitudes, Rossby number less than 1. *Mon. Wea. Rev.*, 96, 197-217.

Krishnamurti, T. N., M. Kanamitsu, W. J. Koss and J. D. Lee, 1973: Tropical east-west circulations during the northern winter. *J. Atmos. Sci.*, 30, 780-787.

Lau, N.-C., 1979: The observed structure of tropospheric stationary waves and the local balances of vorticity and heat. *J. Atmos. Sci.*, 36, 996-1016.

Lau, N.-C., G. White and R. L. Jenne, 1981: *Circulation statistics for the extratropical Northern Hemisphere.* NCAR/TN-171 + STR.,National Center for Atmospheric Research, Boulder, Colorado, 138pp.

Lau, K. M., C. P. Chang and P. H. Chan, 1983: Short term planetary-scale interactions over the tropics and midlatitudes during northern winter. Part II: Winter MONEX periods. *Mon. Wea. Rev.*, 111, 1372-1388.

Murakami, T. and M. S. Unninayar, 1977: Atmospheric circulation during December 1970 through February 1971. *Mon. Wea. Rev.*, **105**, 1024-1038.

Thompson, R. M., S. W. Payne, E. E. Recker and R. J. Reed, 1979: Structure and properties of synoptic-scale wave disturbances in the intertropical convergence zone of the eastern Atlantic. *J. Atmos. Sci.*, **36**, 53-72.
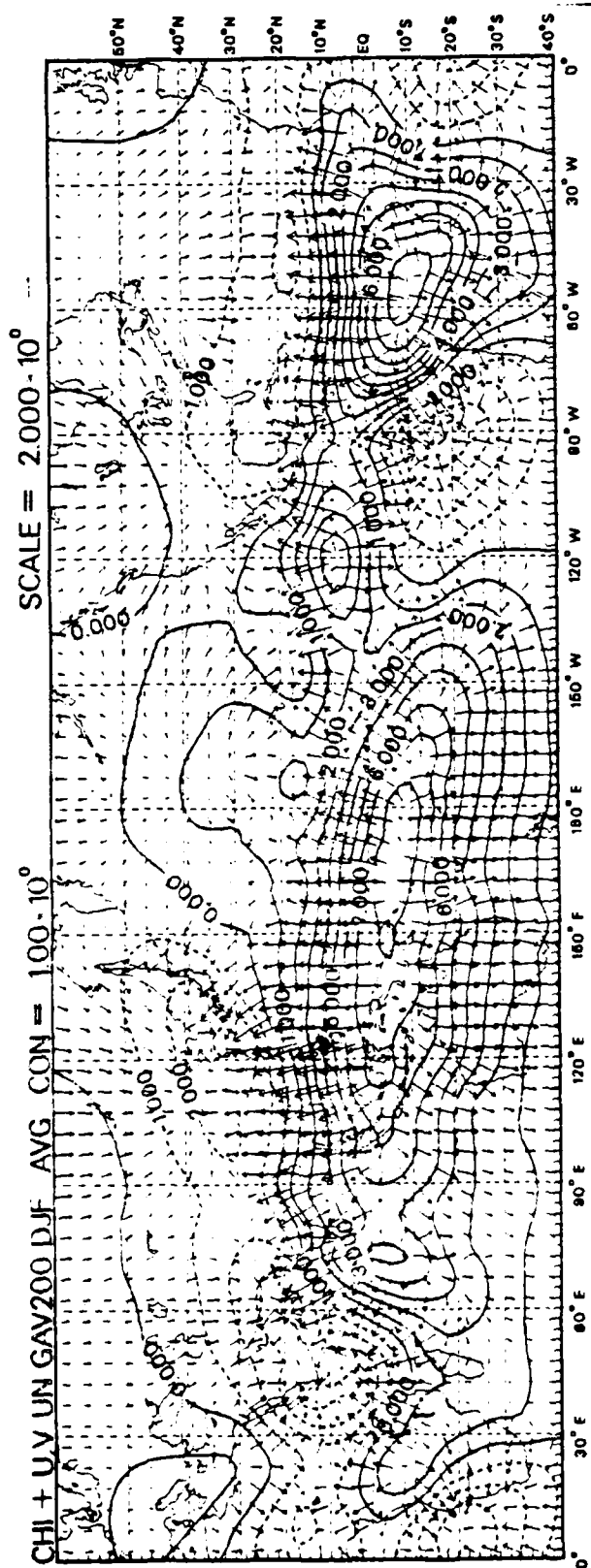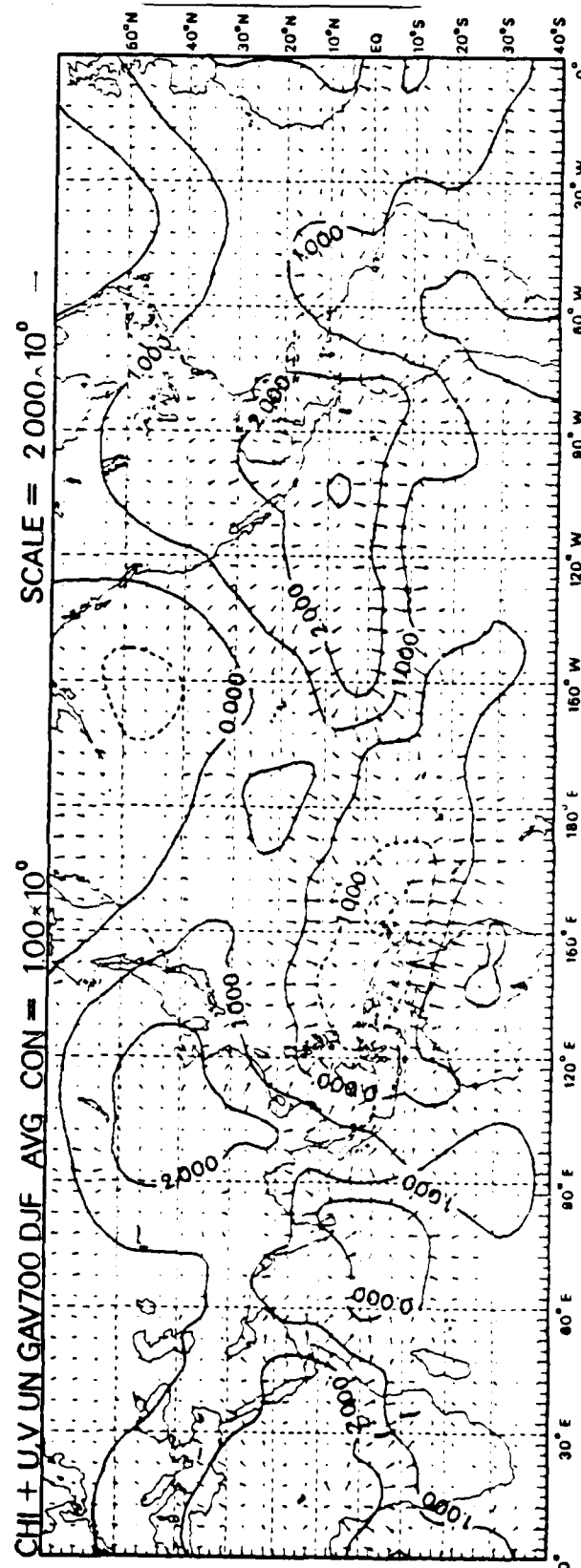
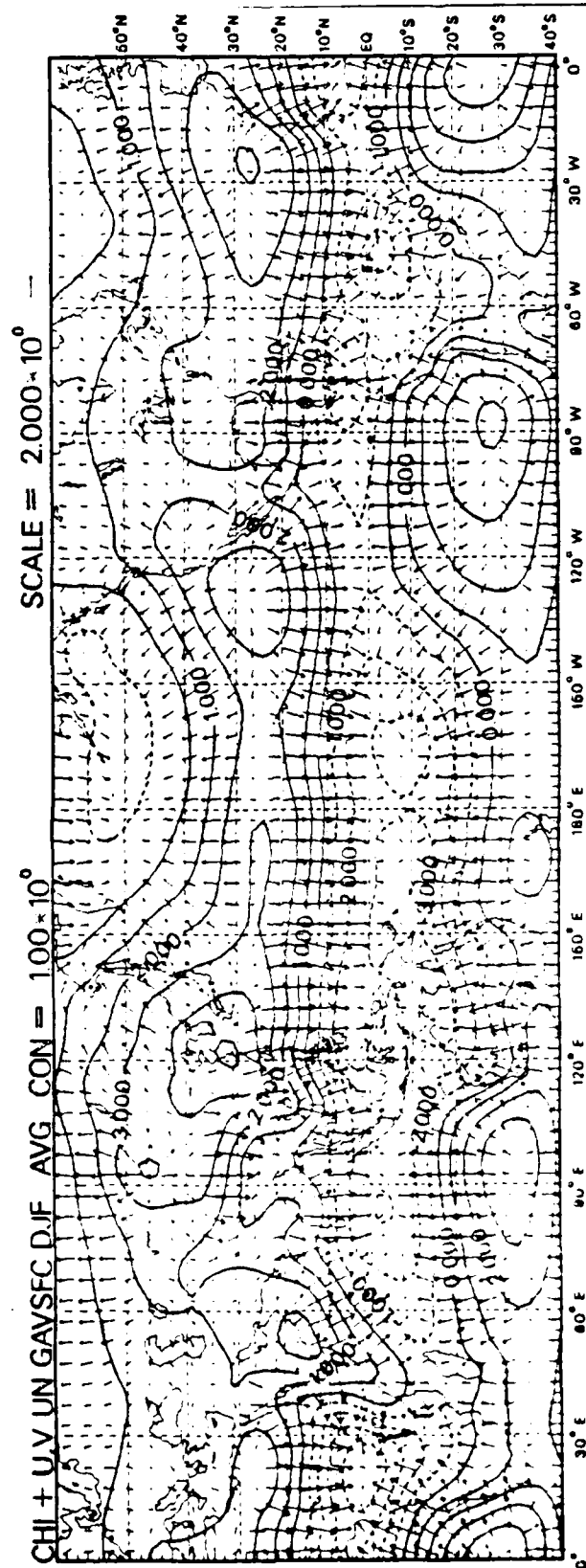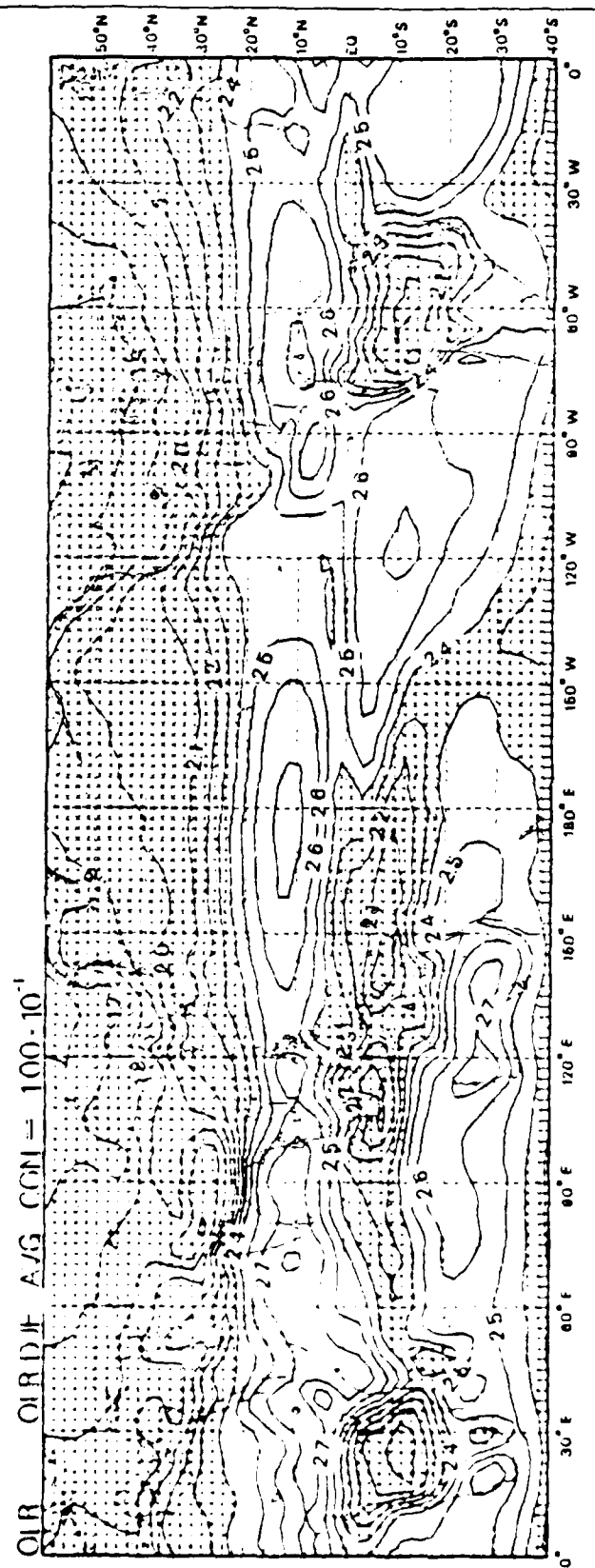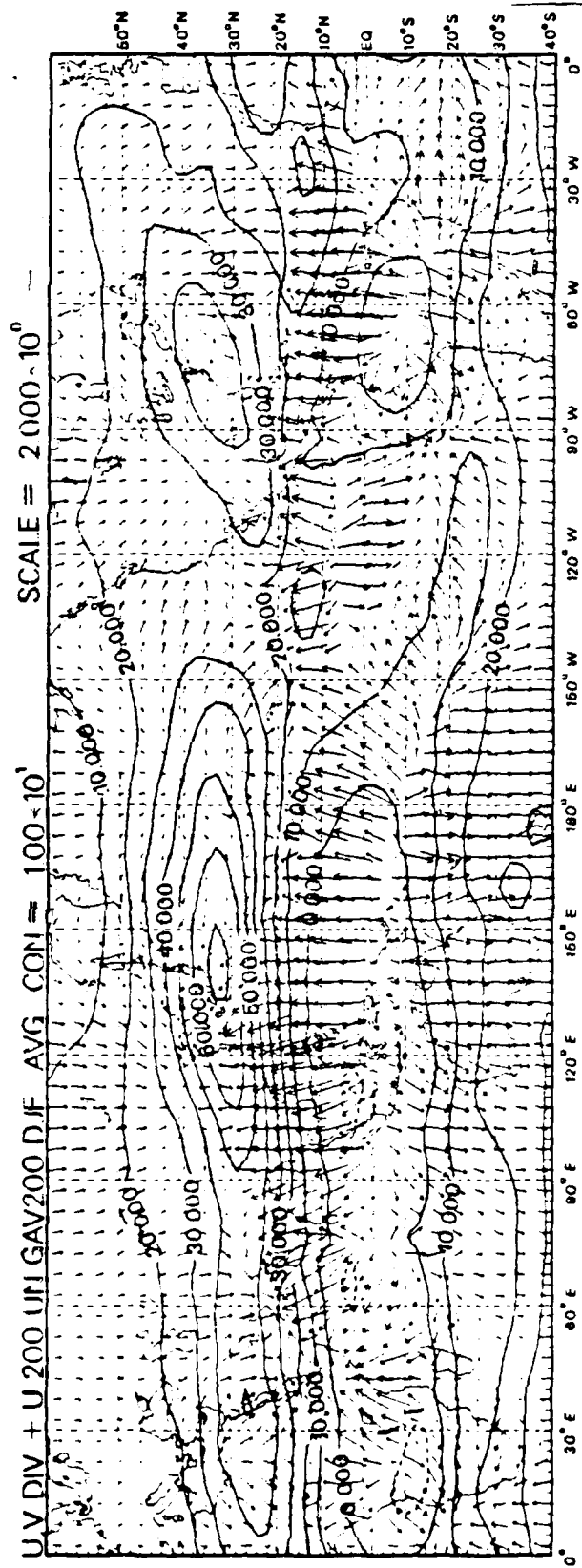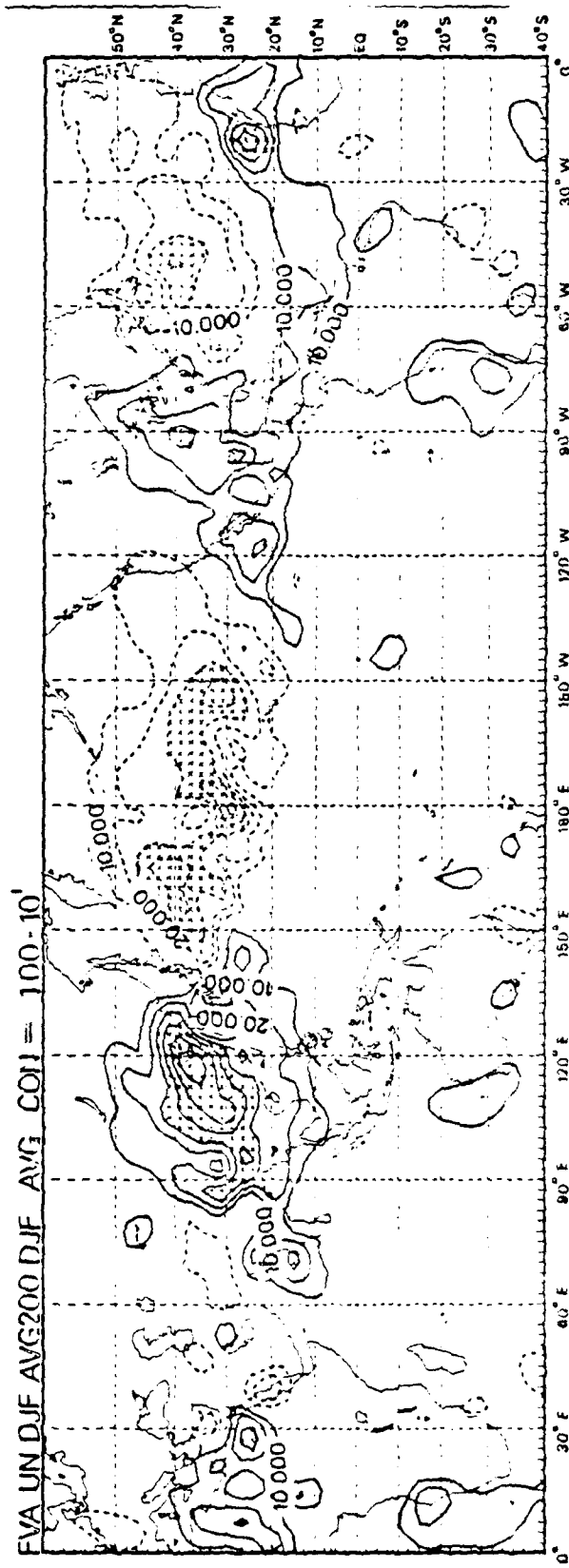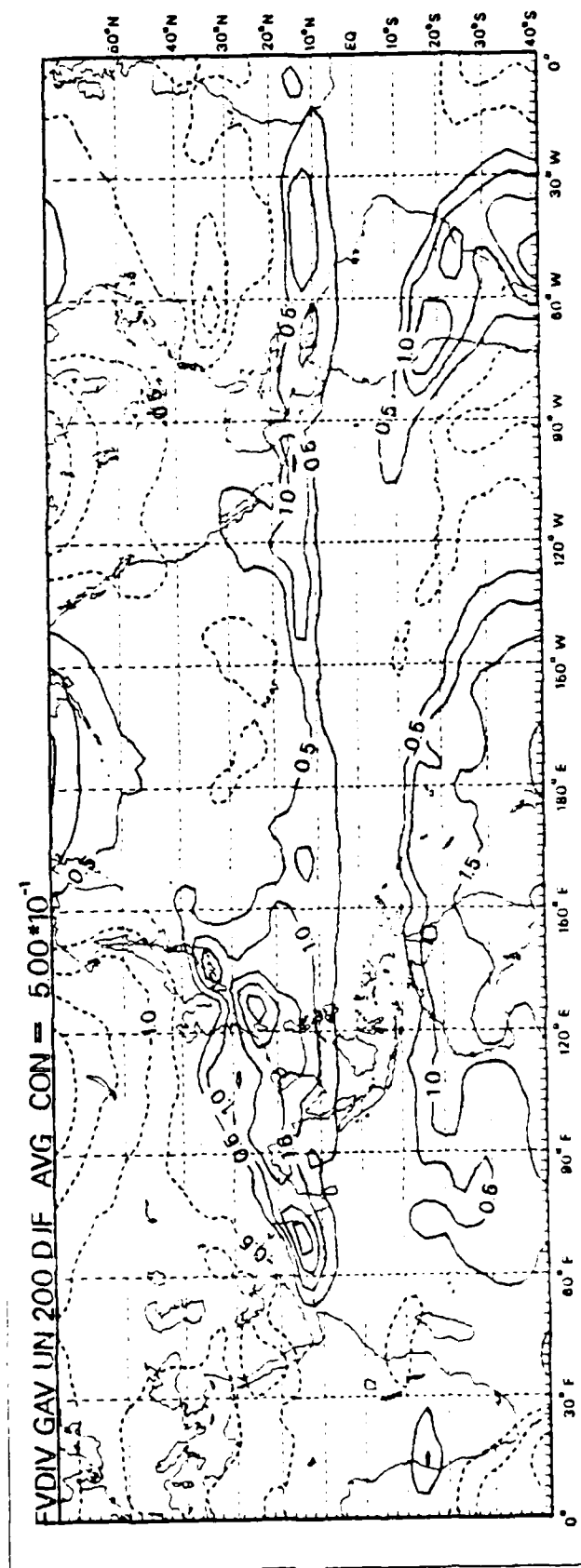CHI + U,V UN GAV200 DJF   AVG   CON = 100·10⁰

SCALE = 2.000·10⁰

Fig. 1A

CHI + U,V UN GAV700 DJF  AVG  CON = 100×10⁰

SCALE = 2 000×10⁰

fig. 1B

73

CHI + U V UN GAVSFC DJF   AVG   CON = 100 × 10⁰   SCALE = 2.000 × 10⁰   ⟶

74

OIR  OIRDIF  A/G  CCN = 100·10⁻¹

Fig. 2

U V DIV + U 200 UH GAV200 DJF   AVG  CON = 100×10¹

SCALE = 2 000×10⁰

FIG. 3

76

EVA UN DJF AVG200 DJF AVG CON= 100-10'

Fig. 4

EVDIV GAV UN 200 DIF  AVG  CON = 5.00*10⁻¹

Fig. 5

78

## ACKNOWLEDGMENTS

# DISTRIBUTION LIST

No. Copies

1. Defense Technical Information Center      2
   Cameron Station
   Alexandria, Virginia 22314

2. Library, Code 0142      2
   Naval Postgraduate School
   Monterey, California 93943

3. Department of Meteorology      1
   Code 63, Naval Postgraduate School
   Monterey, California 93943

4. Professor James S. Boyle, Code 63By      2
   Naval Postgraduate School
   Monterey, California 93943

5. Professor C.-P. Chang, Code 63Cp      2
   Naval Postgraduate School
   Monterey, California 93943

6. Dr. Phil Arkin      2
   Climate Analysis Center
   NOAA/NMC
   **World Weather** Building
   Washington, DC 20233

7. Director of Research Administration      1
   Code 012
   Naval Postgraduate School
   Monterey, CA 93943

END

FILMED

FEB. 1988

DTIC